

The effect of time on the weathering of silicate minerals: why do weathering rates differ in the laboratory and field?

Art F. White^{a,*}, Susan L. Brantley^b

^aU.S. Geological Survey, MS 420, 345 Middlefield Road, Menlo Park, CA 94025, USA

^bDepartment of Geosciences, Pennsylvania State University, University Park, PA 16802, USA

Received 4 December 2001; received in revised form 3 March 2003; accepted 25 March 2003

Abstract

The correlation between decreasing reaction rates of silicate minerals and increasing duration of chemical weathering was investigated for both experimental and field conditions. Column studies, using freshly prepared Panola Granite, produced ambient plagioclase weathering rates that decreased parabolically over 6 years to a final rate of $7.0 \times 10^{-14} \text{ mol m}^{-2} \text{ s}^{-1}$. In contrast, the corresponding plagioclase reaction rate for partially kaolinized Panola Granite, after reaching steady-state weathering after 2 months of reactions, was significantly less ($2.1 \times 10^{-15} \text{ mol m}^{-2} \text{ s}^{-1}$). Both rates were normalized to plagioclase content and BET surface area. Extrapolation of decreasing rates for the fresh plagioclase with time indicated that several thousand years of reaction would be required to replicate the rate of the naturally weathered plagioclase under identical experimental conditions. Both rates would remain orders of magnitude faster than field weathering rates previously measured for a weathering profile in the Panola Granite.

Additional trends in weathering rates with time were established from a tabulation of previously reported experimental and field rates for plagioclase, K-feldspar, hornblende and biotite. Discrepancies in the literature, produced by normalization of weathering rates with respect to surface areas measured by gas absorption (BET) and geometric methods, were overcome by developing a time-dependent roughness factor. Regression curves through the corrected rates produced strong correlations with time that were similar for the four silicate minerals. The average silicate weathering rate R ($\text{mol m}^{-2} \text{ s}^{-1}$) was described by the power function

$$R = 3.1 \times 10^{-13} t^{-0.61}$$

which was similar to the relationship describing the decrease in the fresh Panola plagioclase with time and suggesting control by transport-limited reaction.

The time dependency of silicate weathering is discussed in terms of processes intrinsic to the silicate mineral and those extrinsic to the weathering environment. Intrinsic surface area, which increases with the duration of weathering, was shown to account for a third of the exponential decrease in the weathering rate shown by the above equation. Other factors, including progressive depletion of energetically reactive surfaces and accumulation of leached layers and secondary precipitates, must explain differences for fresh and weathered plagioclase reacting under identical experimental conditions. Extrinsic controls, including low permeability, high mineral/fluid ratios and increased solute concentrations, produce

* Corresponding author. Tel.: +1-650-329-4519; fax: +1-650-329-4538.

E-mail address: afwhite@usgs.gov (A.F. White).

weathering reactions close to thermodynamic equilibrium under field conditions compared to highly unsaturated conditions during experimental reaction of fresh and weathered plagioclase. These differences explain the time-dependent difference in field and lab rates.

© 2003 Published by Elsevier B.V.

Keywords: Weathering rates; Time; Silicate minerals

1. Introduction

Both experimental and field-based approaches have been used to quantify silicate mineral weathering rates at the earth's surface. The advantages of the experimental approach is that chemical, physical and biological conditions are tightly constrained and individual parameters, such as mineral compositions, temperature, surface area, and solute composition, are systematically varied to characterize weathering mechanisms (Lasaga, 1998). The principal disadvantage is that such experiments commonly react freshly prepared silicate minerals over relatively short time intervals, thus producing uncertainties when experimental rates are extrapolated to natural weathering environments.

The alternate approach is to determine long-term mineral weathering rates directly from field studies. Rates are commonly calculated from solute fluxes in soil pore waters, groundwaters and watershed discharge or from changes in solid-state regolith compositions (White and Brantley, 1995 and references therein). Uncertainties in natural weathering rates involve estimating fluid residence times and flow paths, surface areas of complex mineral assemblages and past variations in climate, solute composition and biological activity.

The duration of the weathering process itself, or simply time, is the parameter with the largest variability in the study of chemical weathering. Clearly, the time over which natural chemical weathering occurs, except in a very limited number of environments, (White and Hochella, 1992), cannot be reproduced by experimental studies. Weathering characteristics associated with these different time scales may account for significant discrepancies in silicate weathering rates reported in the literature. Experimental weathering rates for a specific silicate mineral are commonly two to four orders of magni-

tude faster than field-derived rates (Schnoor, 1990; Brantley, 1992; White et al., 1996). In addition, the relative rates at which silicate minerals weather in the laboratory are sometimes different than rates observed in the field. For example, although plagioclase and K-feldspar have comparable laboratory rates (Blum and Stillings, 1995), the field weathering rate of plagioclase is much more rapid than K-feldspar (White et al., 2001).

The effects of time can be seen not only in the discrepancy between experimental and natural weathering rates, but also in systematic decreases in natural rates in progressively older weathering environments. This effect is most directly observed in soil chronosequences in which time becomes the principal independent variable. Commonly in such systems, the rates of primary minerals depletion and secondary clay and metal oxide formation progressively decrease with soil age (Taylor and Blum, 1995; White et al., 1996; Hodson et al., 1999; Stewart et al., 2001).

To date, the relationship between primary silicate reaction rates and the duration of chemical weathering in both experimental and natural systems has not been systematically investigated. This paper addresses this issue by describing ongoing long-term (>6 years) experimental dissolution of plagioclase contained in fresh and weathered granite. This is an effort to bridge part of the time gap between short-term experimental studies and natural weathering and to determine if steady-state rates are achievable under experimental conditions. These rate data are then discussed in the context of time trends derived from an extensive tabulation of laboratory and field-based reaction rates for feldspars, biotite and hornblende. Finally, a review of the time-dependent nature of both intrinsic and extrinsic processes that control weathering rates will be presented.

2. Methodologies

The weathering rate of a silicate mineral, R ($\text{mol m}^{-2} \text{s}^{-1}$), is commonly defined by the relationship

$$R = \frac{Q}{St} \quad (1)$$

where Q (mol) is the moles of a mineral reacted, S (m^2) is the surface area and t (s) is time. In well-stirred flow-through experiments, such as fluidized bed reactors, e.g., Chou and Wollast (1984), the weathering rate can be defined explicitly as

$$R = \frac{(C_o - C_i)}{\beta S} \frac{dV}{dt} \quad (2)$$

where C_i and C_o (mol l^{-1}) are inlet and outlet solute concentrations, β (mol mol^{-1}) is the stoichiometric coefficient describing the number of atoms of solute released per formula unit of the dissolving mineral, and dV/dt is the rate of flow of fluid through the reactor (l s^{-1}). With C_i as a constant, the weathering rate is proportional to the product the effluent concentration and flow rate.

Plug-flow or column reactors have an advantage over stirred and fluidized bed reactors in that they are easily designed as passive gravity flow systems with no mechanical parts, a major consideration for long-term experimental studies. In addition, column reactors are closer analogs to weathering in natural regoliths in which solutes in a volume of infiltrating water progressively react with a continuum of mineral phases.

The disadvantage of column reactors is that Eq. (2) is only an approximation of experimental weathering conditions. Solute gradients are produced in which reactant and product concentrations change with distance within the column, i.e., $C_i - C_o$ is not spatially constant. The measured effluent concentrations reflect only the final pH, mineral solubilities and other conditions that influence and are affected by weathering. In the present study, solute gradients within the columns were minimized by the long duration and slow rates of the reaction that produced very dilute effluent concentrations. Potential pH changes within the columns were buffered by saturating the input solutions with a mixture CO_2/air . In addition, relatively large grain sizes of similar dimensions were used to

produce high porosities and relatively homogenous flow in the column bed.

The columns in this study contained Panola Granite samples obtained from a drill hole penetrating through a deep weathering profile situated on a ridge-top site in the western quadrant of the Panola watershed in the Piedmont province of Georgia, USA. The Panola Granite is classified as a biotite–muscovite–oligo-clase–quartz–microcline granodiorite of Mississippian–Pennsylvanian age. Characteristics of the Panola weathering profile, estimated to be from 200 to 500 ky old, were described in detail elsewhere (White et al., 2001, 2002; White, in press). One sample, composed of pristine granite, was obtained directly beneath the weathering front at 11 m, while a second sample, consisting of partly kaolinized granite, was taken at a shallower depth (8 m) from the same core.

Both the fresh and weathered granite samples were processed through a steel jaw crusher and a ceramic disc mill to obtain a grain size fraction of <2 mm. A relatively coarse subsample (0.25–0.85 mm), obtained by dry sieving, was used to approximate the grain size distributions of the granite. This material was then wet sieved and sonicated to remove fines produced from crushing. SEM observations indicated that this process also removed most, but not all, of the residual clays adhering to the mineral grains in the weathered sample. The granite samples (750 g) were loaded, while wet, into Pyrex glass columns (2.4 cm ID \times 1.0 m length). Distilled deionized water (20 ± 1 °C), saturated with a 5% $\text{CO}_2/95\%$ air gas mixture (input pH=4.5), was introduced through fritted glass supports at the column bases. Flow rates, which averaged 10 ml/h, were controlled by gravity flow through capillary tubes. The effluent discharged through a 0.45-mm filter and into collection bottles. Time-integrated samples, obtained from these bottles, were then chemically analyzed.

Solid-state compositions were determined by X-ray fluorescence analyses (XRF). BET surface area measurements, using multipoint nitrogen isotherms, were made on splits of the column materials at the beginning of the experiments. Additional surface area measurements were made on material removed from the top of the column material after 1.7 and 6.2 years of reaction. Alkalinity and pH were measured using an auto-titrator and solute cations were determined by ICP/MS.

3. Experimental results

3.1. Solid-state characteristics

The compositions of the fresh and weathered granite size fractions used in the column experiments are compared in Table 1 to that of the bulk Panola Granite reported by White et al. (2001). The close correspondence between the bulk granite and the fresh column fractions indicates that size splitting did not selectively enrich or deplete compositions due to mineral grain size differences. In contrast, the naturally weathered column sample is significantly depleted in Na₂O and CaO relative to the bulk granite due to kaolinization of plagioclase (White et al., 2001). Enrichment of MgO and K₂O in the weathered granite was due to preferential retention of micas and K-feldspar during weathering.

The bulk granite averages 26% plagioclase with a composition of An_{0.23} (White et al., 2001). Sodium in the granite is contained almost exclusively in this oligoclase phase. The relative amounts of plagioclase in the fresh and weathered column fractions were established by multiplying the measured percentage in the bulk granite by the ratios of Na₂O in the column samples relative to the bulk granite. Residual plagioclase in the weathered column material (13%) was only half that of the fresh column material (27%).

The specific BET surface area of the fresh and weathered granite column samples measured at the beginning of experiments, and after 1.7 and 6.2 years of reaction are reported in Table 2. As shown in Fig. 1, the surface area of the weathered granite is more than

Table 1
Chemical compositions of Panola Granite (wt.%)

	Bulk Panola Granite	Fresh column fraction	Weathered column fraction
Na ₂ O	3.20	3.29	1.49
K ₂ O	4.53	4.43	5.77
MgO	1.13	0.99	1.30
CaO	2.09	1.93	0.61
Al ₂ O ₃	14.8	14.8	14.7
SiO ₂	66.5	68.2	66.5
Fe ₂ O ₃	4.86	3.82	5.43
TiO ₂	1.00	0.67	1.07
MnO	0.06	0.04	0.06
P ₂ O ₅	0.21	0.19	0.19
Total	98.4	98.4	97.1

Table 2

Surface areas of column materials

Reaction time (years)	Fresh granite (m ² g ⁻¹)	Weathered granite (m ² g ⁻¹)
0	0.084	3.85
1.66	0.126	3.46
6.21	0.298	5.33

an order of magnitude greater than the fresh granite, even through the same grain size fractions were used in both columns. This is due both to increased pitting and surface roughness of the naturally weathered primary silicates as well as to the presence of small amounts of secondary clays that could not be removed during washing and sonification.

The surface area of the fresh granite increases by a factor of about 3.5 after reaction for 6.2 years while the increase in the weathered granite surface area is only a factor of 1.2. The surface area of weathered granite is less affected by additional experimental reaction than that of the fresh granite, which was previously unexposed to weathering.

3.2. Effluent compositions

Representative effluent compositions, produced from the fresh and weathered granite columns, are listed in Table 3. The high Ca concentrations at the beginning of the fresh granite experiment were from

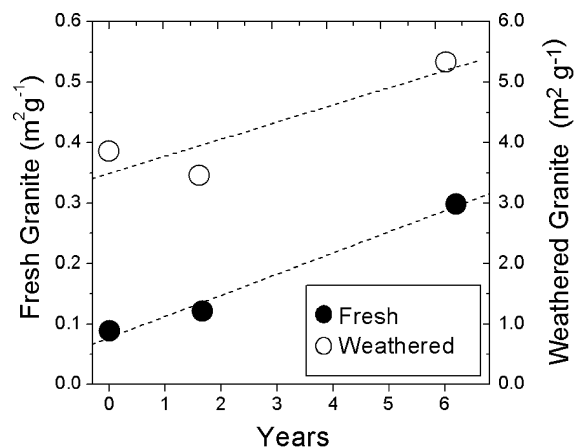


Fig. 1. Changes in BET surface areas of column granite samples as function of the duration of experimental weathering. Dashed lines are linear regression correlations where $S_{\text{fresh}} = 0.078 + 0.035t$, $r = 0.99$, and $S_{\text{weathered}} = 3.49 + 0.28t$, $r = 0.89$.

Table 3
Representative effluent compositions from Panola columns (μM)

Time (years)	Volume (l)	pH	Na	Mg	Al	Si	K	Ca
<i>Fresh Panola Granite</i>								
0.01	0	6.26	18.9	8.70	12.0	46.7	8.31	26.4
0.12	2	6.31	2.43	3.85	1.72	8.10	3.67	11.1
0.60	66	6.05	2.17	0.32	0.77	11.4	1.35	7.53
1.15	116	5.60	2.06	0.07	0.64	8.94	0.61	0.62
3.03	278	5.63	2.41	0.07	0.65	9.10	0.72	0.57
5.30	438	5.71	2.48	0.10	0.79	9.20	0.55	0.55
6.11	544	5.78	2.12	0.18	0.54	10.2	0.63	2.25
<i>Weathered Panola Granite</i>								
0.01	1	6.42	43.2	8.62	0.23	17.3	25.2	6.67
0.11	14	5.72	0.59	3.69	19.1	8.42	2.14	0.50
0.61	66	5.69	0.46	0.12	3.24	6.49	1.30	0.32
1.18	112	5.62	0.46	0.12	3.24	6.49	1.30	0.32
2.90	257	5.65	0.37	0.12	1.18	6.26	0.86	0.41
5.71	463	5.57	0.30	0.09	1.03	5.89	0.95	0.30
6.17	528	5.52	0.33	0.10	1.10	5.00	0.94	0.30

Volume is total flow through columns.

rapid dissolution of trace amounts of disseminated calcite that was depleted with time (White et al., 1999a). This calcite has been previously lost from the naturally weathered granite as is reflected in its lower initial solute Ca concentrations. High initial Si concentrations released from the weathered granite may be attributed to dissolution of secondary silica phases.

Na and Si levels dominate effluents over longer times in the fresh column material, reflecting continued plagioclase dissolution. In contrast, Na is significantly less in effluents from the weathered column, indicating much lower rates of plagioclase weathering. K and Mg concentrations are comparable in both effluents, reflecting the weathering of K-feldspar and biotite. Aluminum levels, higher in effluents from the weathered granite relative to the fresh granite, were attributed to dissolution of secondary clays. The pH of both effluents decreased initially before reaching relatively constant values. The final pH in solutions from the fresh granite (5.8) was slightly higher than from the weathered granite (5.5), reflecting faster rates of silicate hydrolysis. Both pH values are within the range commonly reported for soils and shallow groundwaters.

The effluent Na concentrations from the fresh and weathered Panola Granite, along with the corresponding column flow rates, are plotted against time in Fig. 2. The variations in flow rates reflect gradual clogging of

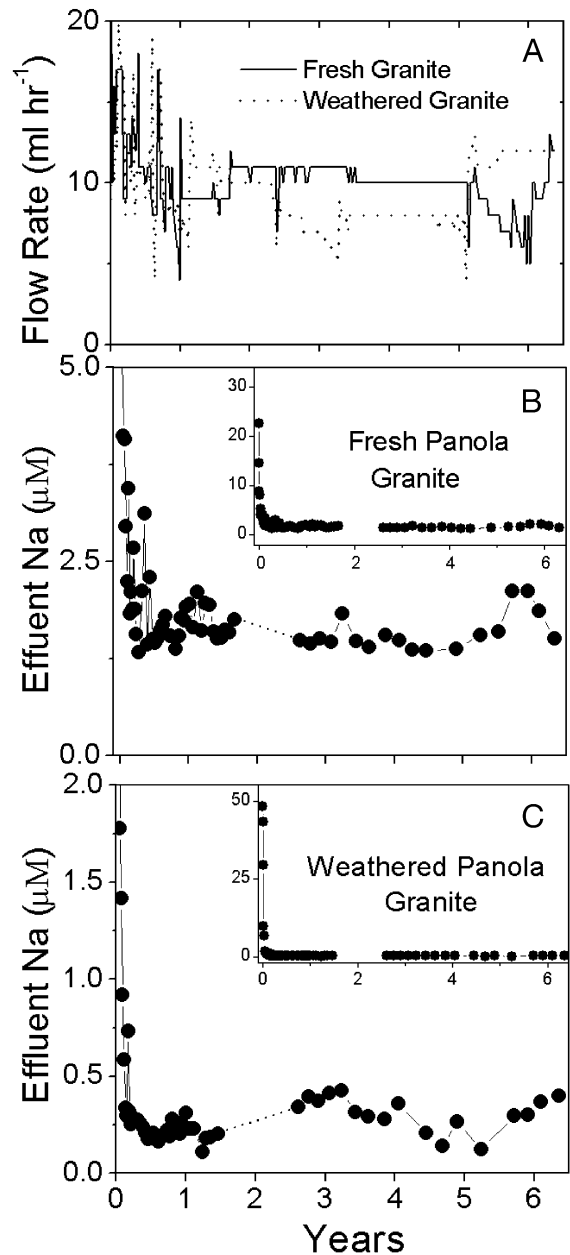


Fig. 2. Flow rates (A) and effluent Na concentrations from the fresh (B) and weathered (C) granite column experiments. Inserts emphasize high solute concentrations associated with the initial stages of reaction. Dotted lines correspond to time period for which data were omitted due to non-ambient temperature conditions.

the capillary tubes over time by mineral precipitates, principally Fe-oxides, and subsequent replacement of the capillaries. This problem was particularly prevalent during early stages of the experiments.

As shown on expanded scales (inserts in Fig. 2B and C), high effluent Na was released during the initial stages of both the fresh and weathered granite experiments. Na concentrations rapidly decreased and reached relatively stable Na concentrations after approximately 2 months of reaction in both columns. The breaks in the data between 1.5 and 2.5 years in both experiments (dotted lines in Fig. 2B and C) correspond to temperature variations of between 6 and 35 °C produced during a study of activation energies for granite weathering (White et al., 1999b). Subsequent Na effluents from the fresh granite experiment, sampled immediately after these experiments, were slightly depressed relative to previous ambient temperature samples and effluents from the weathered columns were somewhat elevated.

Minor Na variability between samplings (Fig. 2) may be due to analytical reproducibility propagated over a 6-year time period. The greater variability for Na in the weathered effluents at long times ($< 10 \mu\text{g l}^{-1}$) is attributed to concentrations approaching an ICP-MS detection limit of 0.1 μM . Additional variability in Na was due to changes in column flow rates. As shown in Fig. 2, lower flow rates generally resulted in increased effluent Na. This is evident in the concentration spike produced in the fresh granite effluent between approximately 5.5 and 6.1 years of reaction (Fig. 2B). This period of time corresponded to a significant decrease in effluent flow rates.

Over long time intervals, effluent Na from the fresh granite remained nearly a factor of 10 higher than from the weathered column. This difference cannot be attributed entirely to the higher Na and plagioclase contents of the fresh granite, which were only a factor of 2 higher than in the weathered granite (Table 1).

3.3. Plagioclase weathering rates

The effluent Na concentrations and flow rates (Fig. 2), along with the BET surface areas (Fig. 1) and the plagioclase stoichiometry, were incorporated into Eq. (2) to approximate plagioclase weathering rates over time (Fig. 3). Calculations assumed that all Na released from the granite is derived from plagioclase,

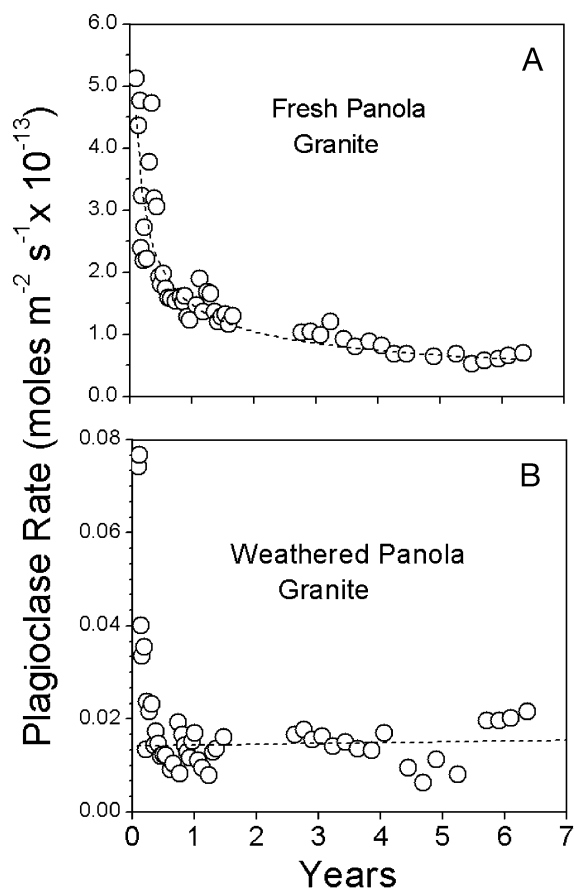


Fig. 3. Plagioclase reaction rates in (A) fresh and (B) weathered Panola Granite as a function of reaction time. Dashed lines correspond to statistical fits to respective data between 0.2 and 6.2 years using power and linear functions (Eqs. (6) and (7)).

which dissolved congruently with a composition of $\text{An}_{0.23}$. Secondly, the surface area of the plagioclase was assumed to be equal to the surface area of bulk granite samples used in the column experiments. In the case of the fresh granite, this was probably a valid approximation because the surface area of the starting material reported in Table 2 ($0.084 \text{ m}^2 \text{ g}^{-1}$) was similar to reported BET surface areas of fresh plagioclase of comparable grain size used in other experimental studies (Table 4).

The extent to which the measured surface area of weathered granite corresponds to plagioclase was more problematic because the potential effects of residual secondary clays and oxyhydroxides with higher surface areas. An initial value of $3.8 \text{ m}^2 \text{ g}^{-1}$

Table 4
Plagioclase weathering rates and related parameters

	Mineral	Rate, log <i>R</i>	Log (years)	pH	Surface measurement	Surface area, <i>S</i> (m ² g ⁻¹)	Grain size (μm)	Roughness, <i>λ</i>	Weathering environment	Reference
1	Albite	-16.4	5.93	nd	BET	1.0 ^a	nd	nd	Solids in Davis Run saprolite, VA, USA	White et al., 2001
2	Oligoclase	-16.3	6.48	6.0–7.0	BET	1.5 ^a	500	331	Solids in China Hat Soil, Merced CA, USA	White et al., 1996
3	Oligoclase	-16.0	5.78	6.0–7.0	BET	1.48	730	477	Solids in Turlock Lake Soil, Merced, CA, USA	White et al., 1996
4	Oligoclase	-15.8	4.00	6.0–7.0	BET	0.26	320	37	Upper Modesto Soil, Merced, CA, USA	White et al., 1996
5	Oligoclase	-15.7	5.40	6.0–7.0	BET	0.46	650 ^a	132	Riverbank Soil, Merced, CA, USA	White et al., 1996
6	Oligoclase	-15.7	5.52	6.0–7.0	BET	0.46 ^a	650	132	Riverbank Soil, Merced, CA, USA	White et al., 1996
7	Oligoclase	-15.7	5.52	6.5	BET	1.0^a	500	221	Panola bedrock, GA, USA	White et al., 2001
8	Oligoclase	-15.5	5.11	6.0–7.0	BET	0.46 ^a	650 ^a	132	Riverbank Soil, Merced, CA, USA	White et al., 1996
9	Oligoclase	-15.1	4.00	6.0–7.0	BET	0.26	320	37	Modesto Soil, Merced, CA, USA	White et al., 1996
10	Oligoclase	-14.9	0.71	5.5–6.4	BET	3.85 (5.33)	250–850	984	Columns, weathered Panola Granite	This study
11	Andesine	-14.7 (-15.3)	4.00	5.0	GEO	0.50 ^a	63–125	nd	Filson Ck. Watershed, MN, USA ³	Siegal and Pfannkuch, 1984
12	Oligoclase	-14.5	0.57	5.0	BET	2.03 (2.78)	10–100	49	Batch reactor, weathered soil	Suarez and Wood, 1995
13	Oligoclase	-14.5 (15.2)	4.00	5.8	GEO	0.50 ^a	63–125	nd	Bear Brook Watershed, ME, USA	Schnoor, 1990
14	Albite	-14.0	0.48	5.5	GEO	nd	0.25	nd	In situ plate dissolution, fresh surface	Nugent et al., 1998
15	Labradorite	-13.7 (15.3)	4.00	6.0–7.5	GEO	0.1200	1–100	nd	Crystal Lake Aquifer, WI, USA	Kenoyer and Bowser, 1992
16	Oligoclase	-13.3 (-15.2)	4.00	3.0–4.5	GEO	0.020	1–4000	nd	Bear Brook watershed soil, ME, USA	Swoboda-Colberg and Drever, 1992
17	Oligoclase	-13.2	0.71	5.7–8.3	BET	0.084 (0.298)	250–850	21	Columns, fresh Panola Granite	This study
18	Oligoclase	-13.1	4.00	6.0	BET	1.53	nd	nd	Gardsjon watershed soil, Sweden	Sverdrup and Warfvinge, 1995
19	Labradorite	-12.9 (-15.3)	5.60	6.0–8.5	GEO	0.030	1000	nd	Rio Parana, Brazil	Benedetti et al., 1994
20	Oligoclase	-12.8	4.00	7.0	BET	0.21	53–208	9	Loch Vale Nano- Catchment, CO, USA	Clow and Drever, 1996
21	Oligoclase	-12.6	-0.39	5.6	BET	0.21	53–208	2	Flow-through column, natural soil	Clow and Drever, 1996
22	Oligoclase	-12.5 (-14.9)	5.50	6.8	GEO	0.003	1000	nd	Coweeta Watershed, NC, USA	Velbel, 1985
23	Albite	-12.5	-2.00	5.6	BET	0.058 (0.074)	74–149	3	Flow-through reactor	Hamilton et al., 2000
24	Albite	-12.1	-0.86	5.0	BET	0.86	125–75	10	Flow-through reactor	Knauss and Wolery, 1986
25	Oligoclase	-12.1 (-14.0)	4.00	5.0	GEO	0.057	nd	nd	Trnavka River watershed, Czech.	Paces, 1986

(continued on next page)

Table 4 (continued)

Mineral	Rate, log <i>R</i>	Log (years)	pH	Surface measurement	Surface area, <i>S</i> (m ² g ⁻¹)	Grain size (μm)	Roughness, λ	Weathering environment	Reference
26 Oligoclase	-12.1	-0.64	3.0	BET	0.33	37–75	19	Batch reactor	Holdren and Speyer, 1987
27 Oligoclase	-12.0	-0.69	5.0	BET	0.20	75–150	4	Fluidized bed reactor	Oxburgh et al., 1994
28 Albite	-11.9	-1.74	5.6	BET	0.08	50–100	3	Fluidized bed reactor	Chou and Wollast, 1984
29 Oligoclase	-11.6	-0.86	5.0	BET	1.01	<37	8	Batch reactor	Busenberg and Clemency, 1976
30 Oligoclase	-11.8 (-13.7)	4.00	nd	GEO	0.030	100	nd	Plastic Lake, Ontario, Canada	Kirkwood and Nesbitt, 1991
31 Oligoclase	-11.8	-0.96	nd	BET	0.2600	53–208	21	Fluidized bed reactor, natural soil	Clow and Drever, 1996
32 labradorite	-11.6	-0.32	5.0	BET	0.11	90–125	8	Flow-through cell	van Hees et al., 2002
33 Oligoclase	-11.6 (-12.2)	-1.09	4.0	GEO	0.50 ^a	63–125	nd	Flow-through columns, natural soil	Schnoor, 1990
34 Oligoclase	-11.4	-0.86	5.0	BET	0.12	125–250	10	Fluidized bed reactor	Mast and Drever, 1987
35 Albite	-11.3	-0.64	6.0	BET	0.11 (0.11)	200–400	3	Flow-through reactor	Holdren and Speyer, 1987
36 Labradorite	-11.3	-0.68	4.0	BET	1.10	38–42	9	Batch reactor	Siegal and Pfannkuch, 1984
37 Albite	-11.3	-1.86	6.0	BET	0.053	125–250	4	Fluidized bed reactor	Welch and Ullman, 1996
38 Oligoclase	-11.2	-0.70	3.0	BET	0.088 (.20)	75–150	4	Flow-through reactor, fresh mineral	Stillings et al., 1996
39 Oligoclase	-10.9 (-12.7)	-0.65	4.5	GEO	0.020	75–150	nd	Fluidized bed reactor, natural soil	Swoboda-Colberg and Drever, 1992
40 Labradorite	-10.7	-0.24	3.2	BET	0.20 (0.20)	43–110	21	Fluidized bed reactor	Taylor et al., 2000a
41 Bytownite	-10.6	-1.29	6.1	BET	0.077	125–250	2	Fluidized bed reactor, fresh mineral	Welch and Ullman, 1993

Panola studies are denoted in bold text. Rate are reported as mol m⁻² s⁻¹. Rates in parentheses are based on estimated surface roughness (Eq. (4)). Surface areas in parentheses were measured after reaction.

nd=not determined.

^a Assumed surface area.

for the weathered granite is somewhat higher than values of approximately 1 m² g⁻¹ for plagioclase separated from granitic sand weathered over comparable time periods (White et al., 1996). Discussions involving the reaction rate for the weathered plagioclase must be tempered by this uncertainty in the surface area. In all probability, the resulting reaction rate represents a minimum estimated value. For both fresh and weathered granites, surface areas were assumed to increase linearly with time as defined by the correlations shown in Fig. 1 (dashed lines).

During the early stages of the experiments, both fresh and weathered plagioclase weathering rates generally tracked large corresponding changes in effluent Na, i.e., initially high rates that decrease rapidly with time. At longer times, the time-dependency of the two rates diverged. Reaction of the weathered plagioclase reaches relative steady-state rates after about 2 months (Fig. 3B) while the reaction rate of the fresh plagioclase continued to decrease. For a given experiment, the variability in reaction rate was less than the corresponding effluent concentration (Fig. 2). Since the

weathering rates are proportional to the product of solute Na and the flow rate, this implies an inverse correspondence between these two parameters. At the end of the experiments, after approximately 6.2 years, the plagioclase weathering rate in the fresh granite column was $7.0 \times 10^{-14} \text{ mol m}^{-2} \text{ s}^{-1}$ and the rate was $2.1 \times 10^{-15} \text{ mol m}^{-2} \text{ s}^{-1}$ for the weathered granite column.

4. Previously reported weathering rates

The plagioclase rates determined for the long-term Panola experiments are compared to a tabulation of previously reported plagioclase weathering rates (Table 4). This compilation is developed in a context that emphasizes the large-scale differences in the reported durations of experimental and natural weathering. When necessary, cited weathering rates were recalculated so as to be presented in consistent units of mass, surface area and time, i.e., $R = \text{mol m}^{-2} \text{ s}^{-1}$ (Eq. (1)). However, no attempt was made to normalize rates relative to differences in cited mineral stoichiometries. Experimental studies indicate that plagioclase weathering rates increase with increasing anorthite content and decreasing pH (Blum and Stillings, 1995). Consequently, plagioclase rate data in Table 4 are limited to albite to labradorite compositions ($\text{An}_{0.0-0.7}$) reacted over a pH range of 3–8. No trends in reaction rates are evident within these composition and pH ranges, implying other variables dominate plagioclase weathering rates.

The listings in Table 4 are ordered in terms of increasing reaction rates. In general, relative slow rates of natural silicate weathering are at the top of the table and fast experimental rates at the bottom. The final experimental rates for the fresh and weathered plagioclase in Panola Granite are denoted in bold type in Table 4. Also denoted is the field rate for plagioclase in the Panola weathering profile calculated by White et al. (2001). This field rate ($2.8 \times 10^{-16} \text{ mol m}^{-2} \text{ s}^{-1}$) is an order of magnitude slower than for the experimental rate for the weathered Panola Granite ($2.2 \times 10^{-15} \text{ mol m}^{-2} \text{ s}^{-1}$) and more than two orders of magnitude slower than the fresh granite ($7.0 \times 10^{-14} \text{ mol m}^{-2} \text{ s}^{-1}$).

Additional rate data for K-feldspar, hornblende and biotite, other minerals common to granitic rocks, are

listed in Tables 5–7. The parameters comprising these data sets are comparable to those of Table 4 and will be used in a later section in a general discussion of the correlation between silicate reaction rates and the duration of weathering.

4.1. Duration of chemical weathering

The duration of silicate weathering in Tables 4–7 ranges over six orders of magnitude from the shortest experimental study (4 days) to the oldest natural regolith (3 million years). The experimental studies generally report the time period required to reach apparent steady-state weathering. Chemical weathering in natural systems involve very different time scales depending on whether changes in solid-state or solute concentrations are measured. Solid-state weathering rates are based on the differences between elemental, isotopic and mineral compositions measured in present-day regoliths and in the assumed protolith. These changes occur over geologic time scales. Such a solid-state approach was used by White et al. (2001) to calculate plagioclase weathering rates based on changes in solid-state Na concentrations in the Panola Granite (Table 4). The ages of older regoliths are most commonly determined from distributions of cosmogenic isotopes, e.g., Panola (Bierman et al., 1995).

The alternate approach in calculating natural weathering rates is based on solute fluxes. These rates in Tables 4–7 commonly employ watershed discharge (e.g., Velbel, 1985) but are also reported for infiltrating soil pore waters (e.g., Murphy et al., 1998) and along groundwater flow paths (e.g., Kenoyer and Bowser, 1992). Such solute fluxes represent contemporary weathering during fluid residence times in the regolith, commonly on the order of years to decades. Over the entire time span of weathering reported in Tables 4–7, many fluid volumes have circulated through these weathering environments. Contemporary rates may not be entirely representative of past long-term weathering rates due to possible changes in climate and other conditions (Cleaves, 1993; White, in press).

A significant number of the natural weathering rates reported in Tables 4–7 are based on discharge fluxes from upland watersheds in North America and Northern Europe that have been exposed to extensive glaciation during the last major ice age. Although no age dates for their geomorphic development are reported,

Table 5
K-feldspar weathering rates and related parameters

Reference no.	Rate, $\log R$	Log (years)	pH	Surface measurement	Surface area, S ($\text{m}^2 \text{g}^{-1}$)	Grain size (μm)	Roughness, λ	Weathering environment	Reference
1	-16.8	5.93	nd	BET	1.0 ^a	nd	nd	Davis Run Saprolite, VA, USA	White et al., 2001
2	-16.8	5.40	6.0–7.0	BET	0.94	650 ^a	270	Riverbank Soil, Merced, CA, USA	White et al., 1996
3	-16.6	6.48	6.0–7.0	BET	0.81 ^a	500	179	China Hat Soil, Merced CA, USA	White et al., 1996
4	-16.4	5.52	6.0–7.0	BET	0.94 ^a	650	270	Riverbank Soil, Merced, CA, USA	White et al., 1996
5	-16.3	5.78	6.0–7.0	BET	0.81	730	261	Turlock Lake Soil, Merced, CA, USA	White et al., 1996
6	-16.1	5.11	6.0–7.0	BET	0.94 ^a	650 ^a	270	Riverbank Soil, Merced, CA, USA	White et al., 1996
7	-15.3	4.00	6.0–7.0	BET	0.26	170	20	Upper Modesto Soil, Merced, CA, USA	White et al., 1996
8	-14.7 (-16.6)	4.10	6.0–7.0	GEO	0.02	53–100	nd	Adams County IL, USA	Brantley et al., 1993
9	-14.2	0.57	5.0	BET	2.03 (2.61)	10–100	49	Experiment, weathered soil, CA, USA	Suarez and Wood, 1995
10	-13.8	4.00	7.0	BET	na	nd	nd	Loch Vale Nano-Catchment, CO, USA	Clow and Drever, 1996
11	-13.3 (-15.2)	4.00	4.5	GEO	0.020	1–4000	nd	Bear Brook watershed soil, ME, USA	Swoboda-Colberg and Drever, 1992
12	-13.3	4.08	5.6–6.1	BET	1.53	nd	nd	Gardsjon watershed soil, Sweden	Sverdrup, 1990
13	-12.9 (-14.8)	3.70	nd	GEO ^a	nd	nd	nd	Shap Granite, England	Lee et al., 1998
14	-12.8	-0.16	5.6	BET	0.16	125–250	13	Flow-through cell	Schweda, 1989
15	-12.4	-0.64	3.0	BET	0.33	37–75	8	Batch reactor	Holdren and Speyer, 1987
16	-12.3	-0.86	5.0	BET	1.52	<37	25	Batch reactor	Busenberg and Clemency, 1976
17	-12.2	-0.47	5.0	BET	0.11	125–250	5	Flow-through cell	van Hees et al., 2002
17	-11.8 (-13.6)	4.00	nd	GEO	0.03	100	nd	Plastic Lake, Ontario, Canada	Kirkwood and Nesbitt, 1991
18	-11.6	-0.41	2.0	BET	0.245 (0.393)	53–106	4	Flow-through cell, weathered feldspar	Lee et al., 1998
19	-11.6	-0.68	4.0	BET	1.1 ^a	38–42	19	Batch reactor	Siegal and Pfannkuch, 1984
20	-11.4	-0.64	5.0	BET	0.176 (0.196)	37–75	4	Flow-through cell	Holdren and Speyer, 1987
21	-10.7 (-12.6)	-0.65	4.5	GEO	0.020	75–150	nd	Fluidized bed reactor	Swoboda-Colberg and Drever, 1992
22	-10.5	-0.50	2.0	BET	0.104 (0.313)	53–106	4	Flow-through cell, unweathered feldspar	Lee et al., 1998

nd = not determined.

^a Assumed.

Table 6
Hornblende weathering rates and related parameters

Reference no.	Rate, $\log R$	Log (years)	pH	Surface measurement	Surface area, S ($\text{m}^2 \text{g}^{-1}$)	Grain size (μm)	Roughness, λ	Weathering environment	Reference
1	–17.0	6.48	6.0–7.0	BET	0.67 ^a	500	179	China Hat Soil, Merced CA, USA	White et al., 1996
2	–16.4	5.78	6.0–7.0	BET	0.67	730	261	Turlock Lake Soil, Merced, CA, USA	White et al., 1996
3	–16.1	5.51	6.0–7.0	BET	0.72	650	250	Riverbank Soil, Merced, CA, USA	White et al., 1996
4	–16.0	5.40	6.0–7.0	BET	0.72	650	250	Riverbank Soil, Merced, CA, USA	White et al., 1996
5	–15.9	5.11	6.0–7.0	BET	0.72 ^a	650	250	Riverbank Soil, Merced, CA, USA	White et al., 1996
6	–15.7	4.60	6.0–7.0	BET	0.34	320	58	Lower Modesto Soil, Merced, CA, USA	White et al., 1996
7	–14.5 (–16.4)	4.00	4.5	GEO	0.020	1–4000	nd	Bear Brook, ME, USA	Swodoba-Colberg and Drever, 1993
8	–14.1 (–16.0)	4.10	nd	GEO	0.02	53–100	nd	Adams County IL, USA	Brantley et al., 1993
9	–13.6	4.00	4.0	BET	1.53	nd	nd	Lake Gardsjon, Sweden	Sverdrup and Warfvinge, 1995
10	–13.0	–0.16	5	BET	0.28	125–250	28	Plug flow reactor	Frogner and Schweda, 1998
11	–12.8	–1.24	4	BET	4.93	37–149	245	Batch reactor	Cygan et al., 1989
12	–12.5	0.05	5.5	BET	0.33 (0.51)	75–150	20	Stirred flow reactor	Givens et al. (unpub.)
13	–12.3 (–14.2)	4.00	nd	GEO	0.03	100	nd	Plastic Lake, Ontario, Canada	Kirkwood and Nesbitt, 1991
14	–11.9	–0.72	4	BET	0.27	250–500	54	Batch reactor	Zhang and Bloom, 1999
15	–11.9	–0.50	4	BET	0.102 (0.3)	110–250	9.6	Batch reactor	Zhang et al., 1996
16	–11.9	–1.09	5.6	BET	0.24	25–30	3	Stirred flow reactor	Nickel, 1973
17	–11.8 (–13.7)	–0.64	4.5	GEO	0.08	75–150	nd	Fluidized bed reactor	Swodoba-Colberg and Drever, 1993
18	–10.7	–1.16	5.5	BET	0.24	33	4.2	Batch reactor	Sverdrup, 1990

Rates are reported as $\text{mol m}^{-2} \text{s}^{-1}$. Rates in parentheses are based on estimated surface roughness (Eq. (4)). Surface areas in parentheses were measured after reaction.

nd = not determined.

^a Assumed surface area.

they are assigned an approximate age of 10 ky, assuming the mineral exposure was initiated immediately after the last major glaciation.

4.2. Normalization by surface areas

Weathering rates in Tables 4–7 are normalized to the surface areas of the reacting silicates (Eq. (1))

based either on gas sorption isotherms (BET) or geometric estimates (GEO). BET values are incorporated into almost all of the experimental rate data with some studies, as in the case of the present Panola study, reporting values before and after reaction (later data in parentheses in the tables).

The difficulty in assessing physical surface areas in the natural weathering environment produces a greater

Table 7
Biotite weathering rates and related parameters

Refer. no.	Rate, $\log R$ ($\text{mol m}^{-2} \text{s}^{-1}$)	Log (years)	pH	Surface measurement	Surface area, S ($\text{m}^2 \text{g}^{-1}$)	Grain size (μm)	Roughness, λ	Weathering environment	Reference
1	–16.5	5.70	5.0–5.5	BET	5	100–500	775	Panola, GA USA	White, 2002
2	–15.5 (–17.4)	4.00	6.0–7.5	GEO	12	1–100	nd	Crystal Lake Aquifer, WI, USA	Kenoyer and Bowser, 1992
3	–15.4	5.48	4.5–5.5	BET	8.1	200–1200	2900	Luquillo, Mtn., PR	White, 2002
4	–15.4	0.57	5.0	BET	8.1 (11.2)	10–100	230	Batch reactor, weathered soil	Suarez and Wood, 1995
5	–15.0	5.48	4.5–5.5	BET	8.1	200–1200	2900	Luquillo, Mtn., PR	Murphy et al., 1998
6	–14.1	4.00	7.0	BET	3.2	nd	nd	Loch Vale Nano-Catchment, CO, USA	Clow and Drever, 1996
7	–14.0 (–15.9)	4.00	4.5	GEO	0.0800	1–4000	nd	Bear Brook, MA USA	Swodoba-Colberg and Drever, 1993
8	–13.2	–0.36	nd	BET	3.2	nd	nd	Loch Vale Soil, flow-through column	Clow and Drever, 1996
9	–13.0	–0.96	5.6	BET	3.2	nd	nd	Loch Vale Soil, fluidized bed reactor	Clow and Drever, 1996
10	–12.9 (–14.8)	5.48	6.0	GEO	0.006	1	nd	Coweeta, NC USA	Velbel, 1985
11	–12.1	–0.94	4.3	BET	5.59 (12.2)	10–20	43	Dialysis cell (fluidized bed)	Kalinowski and Schweda, 1996
12	–11.8	–0.23	4.0	BET	0.84	150–426	273	Column	Acker and Bricker, 1992
13	–11.6	–1.07	3.0	BET	1.28 (1.28)	43–110	51	Flow-through Column	Taylor et al., 2000b
14	–11.5	–1.00	4.0–4.5	BET	1.5300	nd	nd	Fluidized bed reactor	Sverdrup and Warfvinge, 1995
15	–11.4 (–13.3)	–0.64	4.5	GEO	0.08	75–150	nd	Fluidized bed reactor	Swodoba-Colberg and Drever, 1993
16	–11.2	–1.12	5.0	BET	1.81–4.7	75–125	168	Flow-through reactor	Malmstrom and Banwart, 1997
17	–10.7	–0.24	5.0	BET	0.84	150–425	125	Fluidized bed reactor	Acker and Bricker, 1992

Rates are reported as $\text{mol m}^{-2} \text{s}^{-1}$. Rates in parentheses are based on estimated surface roughness (Eq. (4)). Surface areas in parentheses were measured after reaction.

nd=not determined.

variability in measurement methods. Surface areas of soils, saprolites and unconsolidated sediments are commonly characterized by BET methods in a manner similar to experimental material, e.g., Sverdrup and Warfvinge, 1995. Estimating natural mineral surface areas becomes more difficult in weathering environments comprising weathered bedrock, fractures and larger scale weathering environments such as watersheds (Paces, 1973). In such studies, surface areas are commonly based on estimated mineral grain sizes or the distribution of fracture surfaces.

Experimental particle size distributions are generally well characterized and are limited to a narrow size range reported in Tables 4–7. Several studies investigated the effects of particle size on reaction rates, e.g., Holdren and Speyer, 1987, and the selected rate data in the tables correspond to a specific size fraction. In the case of natural weathering, such as in soils, particle size distributions tend to be much larger and less well characterized. Some studies assume that most of the weatherable primary silicates are in the coarse size fractions. Other studies report a single

value, representative of the average of all the grain sizes.

The scale of geometric surface area measurements, using even microscopic techniques such as SEM (Dorn, 1995) and AFM (Brantley et al., 1999), is orders of magnitude greater than the atomic scale of the BET methods. This discrepancy is responsible for consistently higher reported BET surface areas compared to geometric estimates (Tables 4–7). The calculated weathering rates are inversely related to the surface area (Eq. (1)). This difference partly explains why most of the natural rates, based on geometric estimates, are faster than experimental rates based on BET estimates.

Surface roughness is one potential method used to reconcile some of the variability in weathering rates introduced by different methods of measuring surface areas. Surface roughness λ defines the ratio of the BET specific surface area, s_{BET} , to the geometric surface area, s_{Geo} (Helgeson et al., 1984), such that

$$\lambda = \frac{s_{\text{BET}}}{s_{\text{Geo}}} \quad (3)$$

Assuming particles of spherical geometry, the surface roughness λ can be calculated from the BET specific surface area, mineral particle density ρ (g cm^{-3}) and grain diameter D (cm) such that

$$\lambda = \frac{\rho D s_{\text{BET}}}{6} \quad (4)$$

Surface roughnesses were calculated from Eq. (4) for studies that reported both BET surface areas s_{BET} and grain sizes (Tables 4–7). Respective feldspar, hornblende and biotite densities were assumed to be 2.6, 3.2 and 3.0 g cm^{-3} . For studies reporting a range of grain sizes, a mean size was used to determine roughness. Resulting surface roughnesses, averaged from the data in Tables 4–7 for fresh unreacted K-feldspar, plagioclase and hornblende (8.4, 9.2 and 15.1, respectively), are plotted on the left side of Fig. 4. These roughnesses are slightly higher than a previously reported average of $\lambda=7$ for a wide size range of fresh silicate surfaces (White and Peterson, 1990). An average fresh biotite surface roughness of 110 is significantly higher than for the other silicates. This discrepancy is due to the layered structure of mica that is not approximated by spherical surface

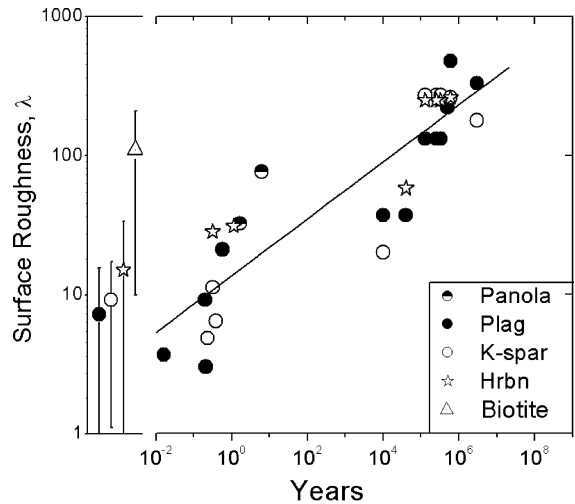


Fig. 4. Silicate surface roughness versus weathering time (data from Tables 4–6). The diagonal line is the fit to the exponential expression given by Eq. (5). Data on left side of figure is average roughnesses (with error bars) for fresh minerals prior to reaction.

geometry (Eq. (4)) and which produces significantly higher BET surface areas than for other silicate phases.

Chemical weathering is shown to significantly increase surface roughness with time due to increasing surface pitting and internal porosity (Anbeek, 1992; White et al., 1996; Brantley et al., 1999). Such increases are plotted as a function of reaction time on the right side of Fig. 4. In the case of experimental weathering, surface roughnesses are calculated from BET surface area measured at the end of each study (data in parentheses in Tables 4–7). Surface roughnesses for the naturally weathered silicates are correlated to the total duration of chemical weathering.

As indicated, feldspar and hornblende surface roughnesses increase significantly with time, approaching values of 800 after a million years of natural weathering (Fig. 4). Within the variability of the data, no significant difference in the time trends for the different minerals exists. Biotite weathers to epitaxial alteration products such as kaolinite, which hinders physical separation. This creates abnormally high BET surface areas and surface roughnesses $\lambda > 2000$ (e.g., Murphy et al., 1998). For this reason, weathered biotite roughnesses are excluded from Fig. 4. The presence of residual clay also explains why the

surfaces of the weathered Panola Granite exhibit anomalously high surface roughnesses (Table 4). In contrast, surface roughness of the fresh Panola Granite, produced after experimental weathering for 1.6 and 6.2 years, are consistent with other silicate minerals (Fig. 4).

If surface roughness increases consistently with time, a standard curve can be constructed such as compiled for hornblende by Brantley and Chen (1995). A regression analysis of the data plotted in Fig. 4, using a power function, produces the relationship between surface roughness and time such that

$$\lambda = 13.6t^{0.20} \quad R = 0.89 \quad (5)$$

which on log-log plot produces a straight line. This relationship can be used to estimate surface roughnesses of silicates for which BET surface area measurements were not made, primarily for those studies investigating field weathering rates. For example, based on Eq. (5), $\lambda=85$ for silicates weathered in watersheds glaciated approximately 10 ky ago (Tables 4–7).

The surface roughness is the ratio of the BET surface area divided by the geometric estimate (Eq. (3)). From Eq. (5), geometric-based weathering rates were converted to equivalent BET-normalized rates based on the estimated duration of chemical weathering. These rates are tabulated in parentheses in Tables 4–7. This approach allowed direct comparisons of weathering rates that were previously irreconcilable and, also, yielded more data in which to investigate weathering trends with time.

5. Discussion

The following sections will investigate in greater detail the relationship between the rates and duration of silicate weathering and will discuss some reasons why time-dependent weathering rates occur.

5.1. Trends in experimental Panola rates with time

A significant difference exists in the response of fresh and weathered Panola plagioclase reaction rates to the duration of experimental reaction (Fig. 3). For the fresh plagioclase, the correlation with time (0.2–

6.2 years) can be described by the power function (dashed line Fig. 3A).

$$R = 1.49 \times 10^{-13} t^{-0.51} \quad (6)$$

The corresponding correlation coefficient and standard errors are reported in Table 8. The negative exponent of -0.51 in Eq. (6) indicates that decrease in the plagioclase weathering rates is essentially parabolic with time.

As previously discussed, the weathered plagioclase rate data exhibit significantly more scatter with time than that for fresh plagioclase. In addition, the magnitude of the surface area is not well established because of the probable influence of residual minerals. In any case, calculated rates for weathered plagioclase, based on measured BET surface areas, do not exhibit a continued parabolic decrease with time, as does the fresh plagioclase (Fig. 3). After a relative short time, the weathered plagioclase rates reach essentially constant values that can be described by the linear rate expression

$$R = 0.0014 + 1.71 \times 10^{-5} t \quad r = 0.0077 \quad (7)$$

which plots as horizontal dashed line in Fig. 3B. Minimal values for the slope and regression coefficient for Eq. (7) indicate a lack of a significant statistical correlation between weathering rate and time for the weathered granite experiment.

Although the fresh plagioclase rate continues to decrease over the course of the experiment, the final rate after 6.2 years of experimental reaction was a factor of 50 times greater than steady-state rate for the

Table 8
Correlations of mineral weathering rates with time for data plotted in Figs. 3 and 6–9

Mineral	Intercept, a_0	Slope, b	Coefficient, r
Fresh Panola plagioclase	-12.83 ± 0.09	-0.509 ± 0.028	0.93
Plagioclase (Table 4)	-12.46 ± 0.16	-0.564 ± 0.046	0.89
K-feldspar (Table 5)	-12.49 ± 0.32	-0.647 ± 0.076	0.83
Hornblende (Table 6)	-12.67 ± 0.22	0.623 ± 0.067	0.92
Biotite (Table 7)	-12.32 ± 0.25	-0.603 ± 0.073	0.83

$$R = a_0 t^b$$

weathered plagioclase (Fig. 3; Table 4). On a log-log plot, Eq. (6), describing the fresh Panola rate, plots as a diagonal straight line with a slope of -0.51 while the estimated steady-state weathered plagioclase plots as a flat line with a slope of zero (Eq. (7)). Extrapolation predicts that the two rates will become equal after approximately 22 ky, a time span out of the realm of experimental verification.

The lack of any apparent variation in the weathered plagioclase experimental rate can also be explained by a parabolic relationship (Eq. (6)) if the duration of experimental reaction is simply viewed as a continuation of previous long-term natural weathering. For example, if natural weathering occurred over 22 ky, the time at which the rates of both experiments would be equal (Fig. 5), an additional increase of 6 years would produce a further decrease in the reaction rate of $<0.01\%$. The argument is therefore advanced that temporal variations in both rates are described by a parabolic decrease (Eq. (6)) but that reaction of weathered plagioclase is much further along on the time curve than is the fresh plagioclase. This weathered rate, however, is still significantly faster than either the field rate (Fig. 5, solid circle) or the extrapolated fresh rate (Eq. (6)) based on the actual age of the regolith (350 ky). This discrepancy suggests that other processes, as will be discussed in a

following section, also suppress natural rates of chemical weathering.

5.2. Trends in literature weathering rates with time

Plagioclase rate data, tabulated from the literature, are plotted as a function of the duration of chemical weathering on a log-log plot in Fig. 6. Experimental data are plotted as open circles with labels corresponding to numerical listings in Table 4. The majority of these experimental rates, plotting in the upper left quadrant of Fig. 6, are based on the dissolution of fresh plagioclase, which, as a group, exhibits no discernible trend between the rate and duration of experimental weathering. This lack of any correlation suggests that difference in mineral compositions and experimental conditions overwhelm any difference in time spans over which the different studies were conducted.

The initial rates of fresh Panola plagioclase dissolution (solid line in Fig. 6) are comparable to short-term fresh plagioclase rates reported in the literature. However, with continued reaction over much longer times, the Panola experiment achieved a final rate (#17, open circle) that was significantly slower than any previously reported value. Except at the very beginning, the weathered Panola plagioclase rates remained consistently slower than literature rates for fresh plagioclase. Interestingly, the final weathered Panola rate (#10, crossed circle) is very similar to a rate reported by Suarez and Wood (1995) for weathered plagioclase from a southern California spodosol that was experimentally reacted for approximately 3 years (Fig. 6, #12). Both rates are normalized with respect to plagioclase content in the regolith and the BET specific surface areas.

For plagioclases, such as from Panola and southern California, the total duration of prior natural weathering greatly exceeds the subsequent experimental reaction times for these minerals. To separate this effect from experimental weathering of fresh counterparts, dashed arrows are included in Fig. 6, which approximate the time span over which natural weathering occurred. In the case of weathered Panola plagioclase (#10), the arrow is projected to the estimated age of the Panola regolith (500 ky). The age of the southern California spodosol (#12) was not reported by Suarez and Wood (1995) but the soil is from a nonglaciated

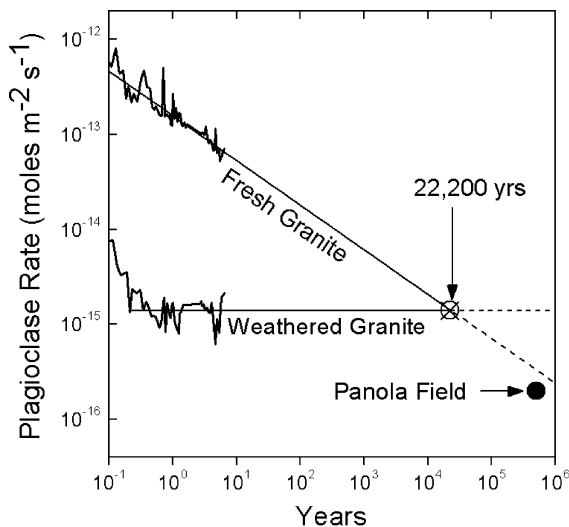


Fig. 5. Extrapolation of experimental plagioclase rates for fresh (Eq. (6)) and weathered (Eq. (7)) Panola Granite. Also indicated is the field rate reported by White et al. (2001).

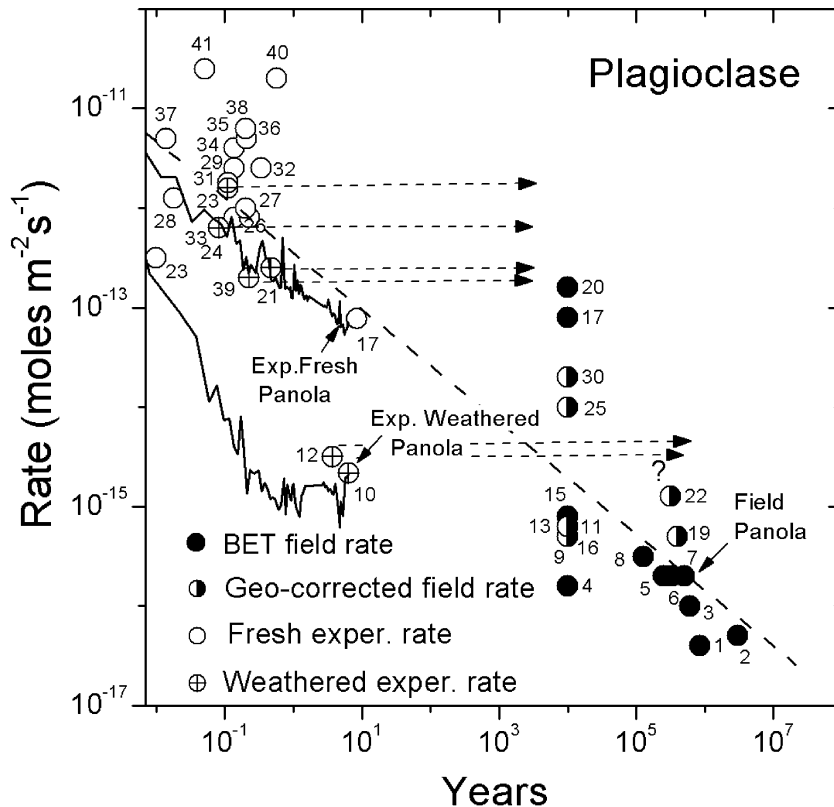


Fig. 6. Experimental and field-based weathering rates of plagioclase as a function of time (data from Table 4). Laboratory rates reflect the duration of experiments. Arrows extend to the approximate ages of naturally weathered plagioclase subsequently subjected to experimental weathering. Field rates reflect the estimated age of the weathering environment. Symbols differentiate between BET-based experimental and BET-based or geometric-corrected field rates. Dashed line is statistical fit to the data based on Eq. (6) (coefficients reported in Table 8).

environment, presumably of comparable age to Panola (dashed arrow with question mark). The remaining experimental studies on naturally weathered plagioclase utilized weathered soils from catchments glaciated in the last 10 ky (Fig. 6; #21, 31, 33 and 39). The corresponding arrows reflect this duration of weathering. As indicated, the experimental weathering for these glacial soils is significantly faster than for the older nonglaciated Panola and California soils.

Plagioclase weathering rates determined from field studies (Table 4) are plotted in Fig. 6 as either closed circles (rates based on BET measurements) or as half-filled circles (rates based on geometric estimates corrected for surface roughnesses). As expected, a significant time gap occurs between the longest-term experimental rates (i.e., Panola) and field weathering rates for the youngest glaciated catchments (10 ky).

Even after corrections for surface roughness, field weathering rates at these young sites, based primarily on watershed discharge, exhibit three orders of magnitude of variation in plagioclase weathering rates. This range probably reflects both actual variations in watershed weathering and uncertainties involved in integrating weathering rates over relative large spatial dimensions. Weathering rates for older weathering environments, spanning 10^2 – 10^3 ky, exhibit significantly less variability, reflecting the fact that these rates are determined from solid-state and solute gradients in generally well-characterized soil and regolith profiles.

In spite of the large number of potential errors and uncertainties associated with a diverse data set (Table 4), a general relationship of decreasing weathering rate with increasing time is clearly evident for plagioclase

(Fig. 6). This trend is quantitatively established by a regression fit (diagonal dashed line) through all the rate data with the exception of the weathered plagioclase from Panola and that of Suarez and Wood (1995). The linear relation of decreasing weathering and increasing time along the log-log axes in Fig. 6 is equivalent to the power function

$$R = 3.47 \times 10^{-13} t^{-0.56} \quad (8)$$

with the correlation coefficient and standard errors reported in Table 8. A close agreement exists between Eqs. (6) and (8), which describes similar time trends observed for the fresh Panola rate data (Fig. 5) and the regression line describing the plagioclase literature rate data (Fig. 7).

The trend established between plagioclase reaction rates and the duration of reaction can be extended to K-feldspar, hornblende and biotite based on data

reported in Tables 5–7. Each mineral exhibits about a six order of magnitude range from the fastest experimental rate to the lowest field rate. The time scales associated with the data are also of comparable magnitude, ranging from less than 4 days for the shortest-term experiment to more than a million years in the oldest natural weathering environment. Although fewer rate data are reported for K-feldspar (21), hornblende (19) and biotite (16), compared to plagioclase (41), relationships of decreasing rates with increasing times are clearly evident in Figs. 7–9.

The dashed diagonal lines plotted in Figs. 7–9 show the regression fits to power functions for K-feldspar, hornblende and biotite rate data that are similar to Eq. (6) for plagioclase. The parameters in Table 8 indicate that these weathering trends with time are statistically valid for all the silicate phases ($r=0.83$ to 0.92). In addition, the pre-exponential

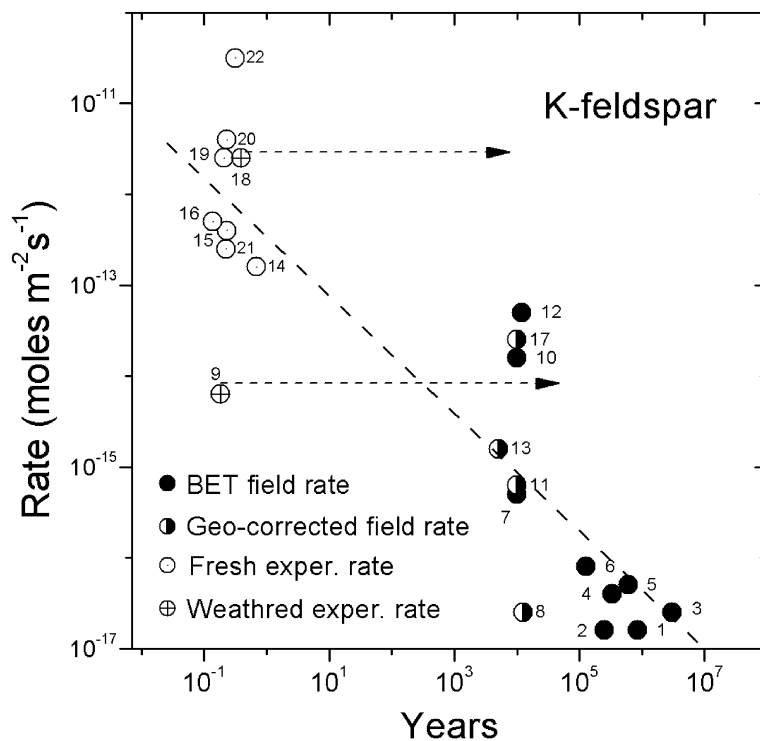


Fig. 7. Experimental and field-based weathering rates of K-feldspar as a function of time (data from Table 5). Laboratory rates reflect the duration of experiments. Arrows extend to the approximate ages of naturally weathered plagioclase subsequently subjected to experimental weathering. Field rates reflect the estimated age of the weathering environment. Symbols differentiate between BET-based experimental and BET-based or geometric-corrected field rates. Dashed line is statistical fit to the data based on Eq. (6) (coefficients reported in Table 8).

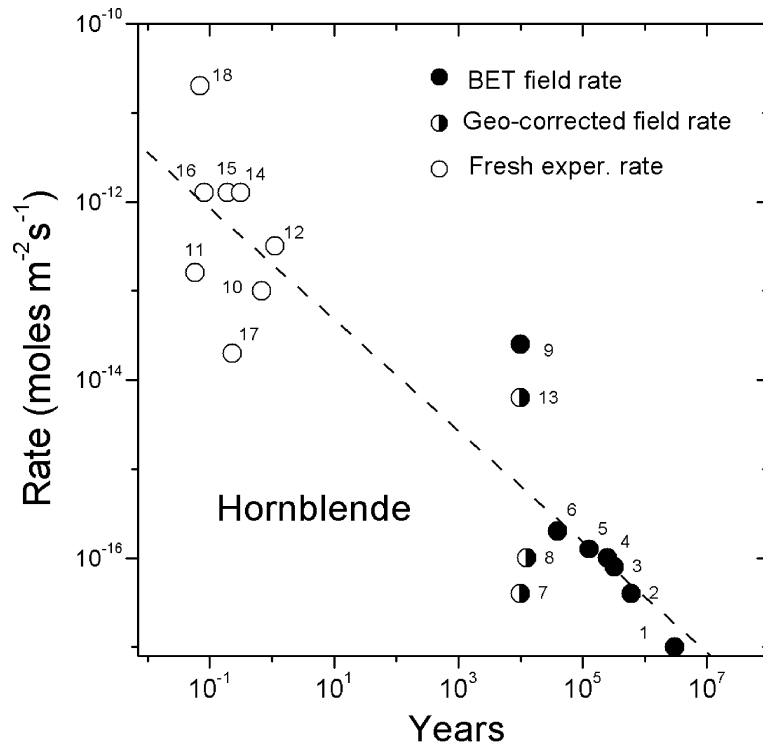


Fig. 8. Experimental and field-based weathering rates of hornblende as a function of time (data from Table 6). Laboratory rates reflect the duration of experiments. Arrows extend to the approximate ages of naturally weathered plagioclase subsequently subjected to experimental weathering. Field rates reflect the estimated age of the weathering environment. Symbols differentiate between BET-based experimental and BET-based or geometric-corrected field rates. Dashed line is statistical fit to the data based on Eq. (6) (coefficients reported in Table 8).

and exponential parameters are essentially identical for all the minerals within the respective margins of errors. The averages of the values for individual mineral rates tabulated in Table 8 produce a general rate expression for silicate weathering at ambient temperature

$$R = 3.1 \times 10^{-13} t^{-0.61} \quad (9)$$

The expression produces a 10-fold decrease in the weathering rate of a silicate mineral after 50 ky, a 100-fold decrease after 2000 ky, a 1000-fold decrease after 10,000 ky, etc. As pointed out by White et al. (2001), such decreases in rate with time explains why silicate minerals persist in the natural weathering environment far longer than predicted from experimental studies.

The similarities in reaction rates over large-scale time, described in Table 8 and summarized in Eq. (9), appear to contradict the long established observation

that different silicate minerals weather at different rates in the field (Goldich, 1938). For example, K-feldspar has been determined to persist over substantially longer times in natural weathering environments than does plagioclase (Banfield and Eggleton, 1990; Nesbitt and Markovics, 1997). However, when the complete range of weathering environments are considered (Tables 4–7), the relative order of reaction becomes less clear. In the case of feldspars, for example, relative rates of plagioclase and K-feldspar vary by less than a factor of 2 under identical experimental conditions (Blum and Stillings, 1995).

The statistical description of the silicate weathering in Table 8 indicates that large-scale time trends in the rate data are clearly evident for each individual mineral. However, the ability to differentiate smaller rate differences between individual minerals reacted over different times is obscured by uncertainties and

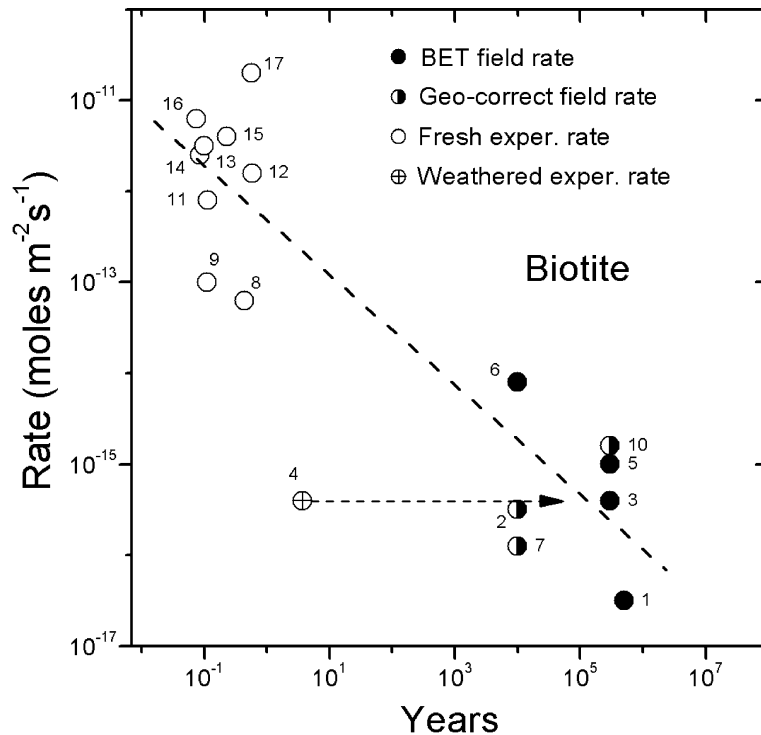


Fig. 9. Experimental and field-based weathering rates of biotite as a function of time (data from Table 7). Laboratory rates reflect the duration of experiments. Field rates reflect the estimated age of the weathering environment. Arrows indicate approximate ages of naturally weathered biotite subsequently subjected to experimental weathering. Symbols differentiate between BET-based experimental and BET-based or geometric-corrected field rates. Dashed line is statistical fit to the data based on Eq. (6) (coefficients reported in Table 8).

errors associated with a wide range of experimental and natural conditions (Tables 4–7).

A power law, comparable to Eq. (9), was developed by Taylor and Blum (1995) to describe the decrease in weathering fluxes from a suite of weathering environments with increasing time. The exponential term used to describe the slope of their data ($b = -0.71$) was slightly steeper than the average of the silicate minerals tabulated in Table 8 ($b = -0.61$). It is interesting to note that Eq. (9) approximates a parabolic expression ($b = -0.50$) commonly used in early experiments to characterize crystalline silicate weathering (Luce et al., 1972) and hydration of natural glasses (Friedman et al., 1994). Although later investigations have discounted diffusion-limited leached layers developing on crystalline silicates at ambient conditions in the laboratory, except at very low pH (Muir et al., 1989; Casey et al., 1993), diffusion-limited weathering under field conditions is possible as will be discussed in the following section.

5.3. Factors affecting the time dependency of weathering rates

A number of processes have been proposed to explain differences between weathering rates observed under both experimental and natural conditions. In terms of their specific time-dependent characteristics, such controls can be classified as being either *intrinsic* or *extrinsic* to a specific silicate mineral (White, 2002). Intrinsic factors are physical and chemical properties of the mineral that may change with time during weathering. Extrinsic features are environmental conditions external to the silicate phase that may also change with time and impact the chemical weathering rate.

Intrinsic properties of the solid phase are generally transferable between weathering environments. For example, if an intrinsic property such as physical surface area is the dominant control on reaction, then experimental measurements of dissolution of previ-

ously weathered minerals should yield rates comparable to those for the natural weathering environment. In contrast, extrinsic properties such as hydrology, solute composition, and biologic interactions are dependent on complex environmental conditions that are difficult to fully recreate under laboratory simulations. Where extrinsic properties control weathering rates, discrepancies between field and laboratory are expected to be the norm. The following sections briefly discuss the role of these intrinsic and extrinsic factors on time-dependent trends in weathering rates.

5.3.1. *Intrinsic weathering properties*

As mentioned above, surface area is an example of an intrinsic characteristic of mineral weathering. On a fundamental basis, weathering rates are dependent on the densities of surface sites at which ligand exchange reactions occur (Casey and Ludwig, 1995). However, in the present study and for the weathering literature cited in Tables 4–7, such surface site densities are assumed to scale directly with the measured physical surface area.

Weathering rates are inversely proportional to surface area (Eq. (1)). Therefore, increases in surface area, due to pitting and etching, are responsible for much of the calculated decrease in weathering rates with time. This effect is shown for the long-term rate data for the fresh Panola Granite, which declines more rapidly than the corresponding measured solute Na levels (Figs. 2 and 3). This is due to normalizing the mass of plagioclase losses by the BET surface areas, which increased by a factor of 3.5 over the course of the experiment. Likewise, the much larger surface areas of naturally weathering silicates, compared to freshly prepared silicates, are partly responsible for the correspondingly lower weathering rates (Tables 4–7).

The extent to which weathering rates scale directly with physical surface area is a matter of considerable debate (White and Peterson, 1990; Brantley et al., 1999). For unsaturated environments, such as in most soils, the surface areas exposed to active fluid transport may be considerably less than the physical surface area of the mineral grains (Drever and Clow, 1995). Surface areas of microscopic features such as external pits and internal pores may be associated with stagnant water that is thermodynamically saturated

and not actively involved in weathering reactions. Finally, Gautier et al. (2001) proposed that much of the measured increase in BET surface area during weathering consisted of increases in essentially unreactive walls of etch pits that contributed negligibly to mineral dissolution. For the above scenarios, the reactive surface area becomes decoupled from the measured physical surface area.

Based on such findings, some workers have suggested that geometric rather than BET surface areas may be more representative of reactive surface areas in the weathering environment (White et al., 1996; Gautier et al., 2001; Mellott et al., 2002). If such a situation is true, the question is raised as to whether the large apparent decreases in weathering rates with time observed in Figs. 4–7 are artifacts based on a normalization using BET measurements which overestimate actual increases in reactive surface area with time.

This issue can be addressed by considering the relative changes in weathering rates and BET surface area with time. Surface roughnesses increase by approximately two orders of magnitude over a million years of weathering (Fig. 4) while the weathering rates decrease by close to six orders of magnitude (Figs. 6–9). The effect of increasing surface area can be quantified by multiplying the reaction rate by the surface roughness which has the effect of negating the surface area normalization, i.e., the trend in rate with time is no longer surface area dependent. This is mathematically equivalent to summing the exponents in Eqs. (5) and (9) such that the resulting function describing the decrease in rate with time contains an exponent of -0.41 rather than -0.61 . This indicates that about a third of the decrease in weathering with time is attributed to concurrent increases in physical surface area while two thirds of the rate decrease must be related to other time-dependent factors.

In addition to the physical surface area, weathering rates are also dependent on temporal changes in intrinsic chemical and structural mineral properties. Examples include the commonly observed preferential weathering of the calcic cores of plagioclase (Clayton, 1986) and perthitic twinning, which often produces spectacular weathering morphologies in alkali feldspars (Lee et al., 1998). With time, selective weathering will diminish the concentration of these

more reactive features, leading to a decrease in overall mineral weathering rate.

Silicate minerals also contain structural defects and dislocations, which represent sites of anomalously high surface energy. If mineral grains are covered by surfaces with high defect densities produced, for example, by natural or laboratory grinding, then with continued weathering, these layers may be removed, leaving behind a less defective surface that weathers at a lower rate (Brantley et al., 1986; Blum and Lasaga, 1987). In fact, in natural systems, weathering may occur predominantly at such defect sites whereas in experimental systems, weathering may occur over the whole mineral surface. As etch pits or etched lamellae get deeper, solution chemistry within the pit may move closer to saturation with respect to the dissolving phase as compared to the bulk solution, slowing the etching process. Consistent with this hypothesis, several workers have documented secondary mineral precipitates within pores developed on weathered silicates, e.g., Yau (1999).

Surface leached layers, secondary mineral precipitates and sorbed organic compounds may also decrease mineral surfaces and, with time, decrease weathering rates. Leached layers have been documented on feldspar weathered in spodosols (Nugent et al., 1998) and on naturally weathered hornblende (Mogk and Locke, 1988). However, other studies have failed to detect leached layers on other naturally weathered silicate substrates (Berner and Holdren, 1977).

The progressive occlusion of the reactive mineral substrate, principally by clays and Fe- and Al-oxides during natural weathering, has been observed (Banfield and Barker, 1994; Nugent et al., 1998). The extent to which secondary minerals produce surface coatings may depend on the degree to which elements are immobilized and the volume ratio of the reactant to product mineral phases (Velbel, 1993). In addition, natural silicate surfaces may become occluded by organic precipitates (Tisdall and Oades, 1982). With time, these effects produce slower diffusion-limited transport of reactants to and products from the reactive substrate. The development of such transport-limited boundaries is suggested by the exponential decrease in the weathering rates with time (Figs. 6–9), which approximate a parabolic diffusion-controlled mechanism.

5.3.2. Extrinsic weathering properties

Changes in large-scale extrinsic features such as climate and biology can affect weathering rates over the long time spans associated with natural weathering (White and Blum, 1995; Moulton and Berner, 1998). However, such processes are not expected to lead to the systematic decreases in reaction rates with time documented in the present study. Rather, the most likely candidates include extrinsic differences in short-term experimental and long-term natural weathering conditions or changes produced by increases in natural weathering intensities with time.

Specific solute species, such as hydrogen ion, Al, Na and organics, have been shown to directly impact silicate weathering rates by aiding or retarding ligand exchange processes at silicate surfaces (Welch and Ullman, 1993; Oelkers et al., 1994; Stillings and Brantley, 1995; Chen and Brantley, 1997). The influence of solute compositions on silicate weathering rates can also be related to their control on the thermodynamic saturation state of the solid phase. Studies involving experimental dissolution of feldspars (Burch et al., 1993; Oelkers et al., 1994; Taylor et al., 2000a) have shown correlations between decreases in dissolution rates as solutes approached to thermodynamic saturation with respect to the reacting phase.

The relationship between weathering rate R and saturation state can be quantitatively expressed using transition state theory (Lasaga, 1998)

$$R = -k_1 \left[1 - \exp \left(-n \frac{\Delta G_r}{R' T} \right)^a \right] - k_2 \left[1 - \exp \left(- \frac{\Delta G_r}{R' T} \right) \right]^b \quad (10)$$

ΔG_r (kcal) is the reaction affinity that describes the extent to which the solute is in thermodynamic disequilibrium with respect to the solid phase, i.e., $\Delta G_r = -RT \log \text{IAP}/K_s$ where IAP is the ionic activity product and K_s is the solubility constant. The weathering rate R is the sum of two parallel reactions. The first term in Eq. (10) contains the rate constant k_1 , which defines fast dissolution far from equilibrium. This reaction is proposed to be driven by the development of etch pitting at dislocation outcrops on the mineral surface (Lasaga and Blum, 1986). The second term, i.e., k_2 , describes the slower rate as the solution

approaches equilibrium and the reaction becomes controlled by the bulk dissolution of the mineral surface.

The transition from far to close to equilibrium reactions has importance ramifications as to the role of fluid transport on chemical weathering. For dilute conditions, Eq. (10) predicts reaction rates are interface-limited and independent of fluid concentrations and rates of solute transport. This situation is generally confirmed for experimental batch reactors with high fluid to mineral ratios in which the weathering rate is independent of the fluid stirring rate.

In contrast, at low reaction affinities, as solute concentrations approach equilibrium, rates will be transport-limited. Increasing flow rates will decrease solute concentrations and saturation states and increase the weathering rate. In general, column experiments employ significantly lower fluid to mineral ratios than batch reactors. [van Grinsven and van Riemsdijk \(1992\)](#) made the case for transport-controlled weathering in soil columns by showing that reaction rates

increased with the increasing percolation rate of solution. [Clow and Drever \(1996\)](#) also found that weathered plagioclase reacted an order of magnitude slower in column experiments than in fluidized bed reactors ([Table 4](#), #21 versus #31) and attributed this difference to stagnant flow regimes in the columns in which mineral surfaces were effectively isolated and were saturated with respect to the reacting mineral.

However, a case of transport-controlled reaction cannot be made for the present Panola column study because of inverse correlations between flow rate and solute concentration as reactions approach steady-state ([Fig. 2](#)). This resulted in a relative consistent reaction rate that appeared not to be transport-limited. This conclusion is supported by the observation that column effluents remained far from thermodynamic saturation with respect to plagioclase ([Fig. 10](#)).

Hydrologic heterogeneity becomes greater as silicates weather in natural environments. A number of workers have attributed variations in natural weathering rates to differences in the hydrologic environment

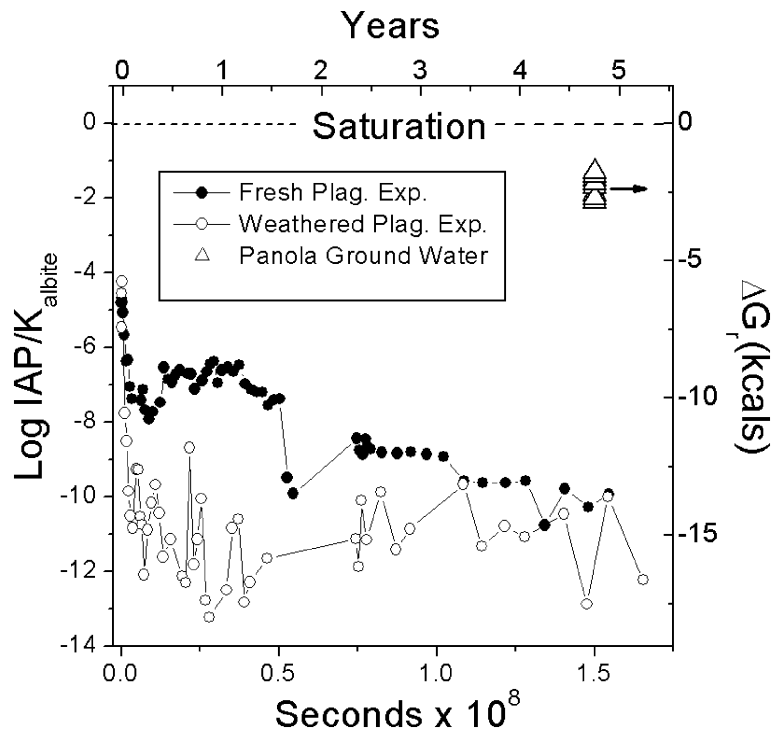


Fig. 10. Saturation states for albite (IAP/K_s) and Gibbs free energy of dissolution for effluents from the fresh and weathered columns versus experimental reaction times. Also plotted, as a time-independent parameters, are the Panola groundwater saturation states (from [White et al., 2001](#)). Thermodynamic conditions are based on the dissolution reaction $\text{NaAlSi}_3\text{O}_8 \rightarrow \text{Na}^+ + \text{Al}(\text{OH})_4^- + 3\text{H}_4\text{SiO}_4$.

(Schnoor, 1990; Swodoba-Colberg and Drever, 1993; Velbel, 1993). Fluid flow becomes highly differentiated with rapid movement through macropores and much slower movement through micropores in the soil matrix (Hornberger et al., 1990). Also, with continued soil weathering, progressively more intense argillic horizons are formed which effectively slow water movement (Smeck and Ciolkosz, 1989), thus increasing solute concentrations and decreasing reaction affinities. Cyclic wetting and drying may cause intermittent rather than continuous weathering and may enhance the irreversible binding of organic polymers to silicate surfaces (Letey, 1984). Finally, mass redistributions produced from chemical weathering substantially impact regolith porosities and water contents, potentially changing unsaturated conductivities and fluid residences by orders of magnitude (Stonestrom et al., 1998).

As the result of these hydrologic processes, thermodynamic calculations show that a significant number of soil and groundwaters approach thermodynamic saturation with respect to primary silicate minerals (Gislason and Arnorsson, 1990; White, 1995; Stefansson, 2001). In addition, Lee et al. (1998) proposed that the time dependence of weathering reactions is further enhanced by the fact that natural weathering, which occurs closer to equilibrium, is more dependent on structural heterogeneities, which continue to dissolve relatively close to saturation.

5.4. Interpretation of the Panola plagioclase rate data

At the end of column experiments, fresh plagioclase weathers more than an order of magnitude faster than weathered plagioclase ($10^{-13.2}$ versus $10^{-14.6}$ mol $m^{-2} s^{-1}$). This difference in rates occurs in spite of identical experimental conditions and after normalizing for mineral content and specific surface area. In addition, the experimental rate of weathered plagioclase is an order of magnitude faster than the field rate for the same granitic material ($10^{-15.6}$ mol $m^{-2} s^{-1}$; White et al., 2001). These differences between experimental weathering rates and between experimental and field rates can only be explained by a combination of both intrinsic and extrinsic weathering controls.

White et al. (2001) made a strong case for near-thermodynamic saturation of groundwaters associated with feldspar weathering in the Panola Granite. Cal-

culations showed that K-feldspar was essentially saturated ($IAP/K_s=0$), and albite, assumed to thermodynamically approximate Panola oligoclase, was slightly undersaturated ($\log IAP/K_s=-1$ to -2). These data are plotted in Fig. 10 both as functions of saturation indices and reaction affinities. These conditions are compared to albite saturation in column effluents calculated using the PHREEQE speciation code (Parkhurst, 1997). As indicated in Fig. 10, initially, the fresh plagioclase effluent is closer to thermodynamic saturation than is the weathered plagioclase effluent due to higher solute concentrations. At progressively longer times, the saturation states of both effluents become comparable and, compared to field conditions, were strongly undersaturated with respect to plagioclase ($\log IAP/K_s \leq -10$).

The final saturation states of the column effluents, calculated as reaction affinities ΔG_r , are plotted against the corresponding reaction rates in Fig. 11. Also plotted is the average value for the Panola groundwater and the

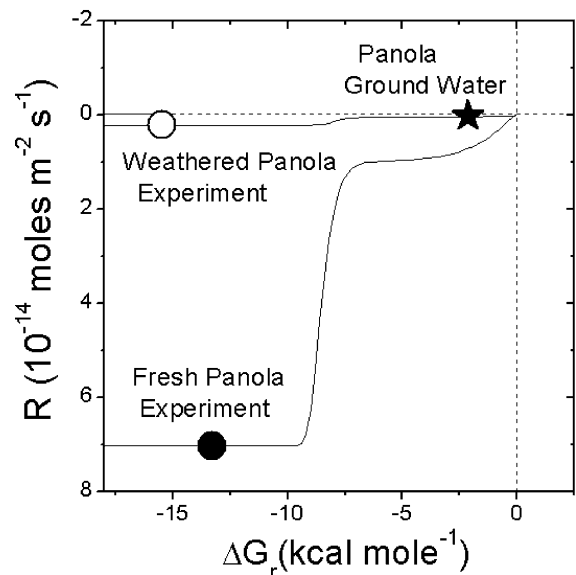


Fig. 11. Reaction rates for fresh and weathered Panola Granite experiments and the field rate for the Panola regolith versus Gibbs free energy of albite dissolution. Solid lines are fits of Eq. (10) to the experimental data. Intersection of dashed lines denotes zero reaction rate at thermodynamic equilibrium. For fresh plagioclase $k_1 = 1.17 \times 10^{-13}$, $k_2 = 1.00 \times 10^{-14}$, $n = 8$. For weathered plagioclase, $k_1 = 1.64 \times 10^{-15}$, $k_2 = 4.6 \times 10^{-15}$ and 5.0×10^{-16} . For both fits, $n = 8 \times 10^{-17}$, $m_1 = 15$ and $m_2 = 1.45$, which are the same values used by Burch et al. (1993).

best fits for Eq. (10) through the experimental rate data. This plot is equivalent to those produced by Burch et al. (1993) and Taylor et al. (2000a) to describe the saturation state effects on experimental plagioclase dissolution. The parameters used to fit the Panola data are listed in the figure caption (Fig. 10). The most sensitive parameter in Eq. (10) is the far-from-equilibrium rate term k_1 which is 1.7×10^{-13} and 4.6×10^{-15} mol $m^{-2} s^{-1}$, respectively, for the fresh and weathered plagioclase. These values closely approximate the respective experimental rates, indicating the lack of saturation control in the column experiments.

The reaction affinities for the column effluents ($\Delta G_r = -13.3$ and -15.6 kcal) are significantly below the threshold energy of -10 kcal, a value at which inhibition of etch pit formation is proposed to occur (Burch et al., 1993; Taylor et al., 2000a). In contrast, the free energy of dissolution for groundwater in contact with the Panola Granite is much closer to equilibrium (-2.6 kcal/mol), suggesting slower reactions on the mineral surface not characterized by nucleation and growth of etch pits. This difference in the saturation state and reaction affinities between experimental and field conditions can explain the differences in respective laboratory and field rates for the weathered feldspar. Since both mineral phases are presumed to be similar in terms of surface area, leached and product layers and other intrinsic features; the large difference in rates is attributed to extrinsic controls, i.e., differences in solute concentrations and saturation states. Presumably higher saturation states in field settings are related to hydrologic and chemical characteristics of in situ weathering over long times.

In contrast, these extrinsic controls cannot explain why the fresh Panola plagioclase weathers faster than weathered plagioclase in the laboratory since the saturation states are comparable (Figs. 10 and 11). The difference in experimental rates implies intrinsic differences in the plagioclase minerals undergoing weathering. These features may include isolation of the reactive surface by development of leached layers, decreased access to dislocation outcrops on the mineral surface after long-term natural weathering or increased dislocation density caused by grinding of fresh surfaces. In summary, a combination of both time-dependent intrinsic and extrinsic controls are required to explain chemical weathering of the Panola Granite over a range of experimental and natural conditions.

6. Conclusion

In conducting the longest running experiment of silicate weathering reported to date (>6 years), this study demonstrated that the reaction of freshly crushed Panola plagioclase never reached steady-state reaction rates. Rather, rates were described by a power function, predicting an essentially parabolic decrease with time. In contrast, experimental reaction of previously weathered granite exhibited relatively constant rates after several months. These results indicate that pre-conditioning by natural weathering significantly decreases both magnitude of the subsequent experimental rate as well as any decrease in rate with additional reaction time. Extrapolation indicates that several thousand years of experimental reaction is required to achieve similar rates for the fresh and weathered samples. Even after such extended reaction, these rates would remain an order of magnitude slower than previously determined field rates for the Panola Granite regolith.

The Panola plagioclase rates are placed in the context of other experimental and field plagioclase rates reported in the literature which spanned time periods ranging from several days for experimental weathering to millions of years for field-based weathering. In order to reconcile significant differences in reported rates to the normalizations by either BET- or geometric-based surface areas, a curve describing the change in roughness with time was generated. Multiplying the geometric surface area by this roughness factor, which reflects increases in etching and pitting with increasing weathering intensities and time, produced corrected geometric rates that were comparable to BET-normalized rates.

A power function, describing the correlation between reaction rates and times from more than 40 experimental and field studies, was very similar to that describing experimental weathering of fresh Panola plagioclase. The nature of this rate–time relationship predicts that rates will initially decrease rapidly during the initial stages of weathering as was observed experimentally for the fresh Panola Granite. However, at long times, the change in weathering is much less, which explains why experimental reaction of the previously weathered Panola Granite exhibited pseudo-steady-state rates.

Construction of similar rate–time relationships for other minerals common to granite rocks, i.e., K-

feldspar, hornblende and biotite, also produced similar trends. These similarities indicated that the time effects on silicate weathering is comparable, both over a large range in the durations of weathering, as well as for a variety of silicate minerals. The exponential decrease in rates with time also explains why silicate minerals persist in the natural weathering environment far longer than predicted by experimental studies.

The time-dependent nature of silicate reaction rates reflects a number of processes reflecting both intrinsic characteristics of the mineral as well as extrinsic features of the weathering environment. Intrinsic effects include increases in physical surface area due to surface roughening, concurrent decreases in reactive surface area due to diminishing compositional and structural heterogeneities, and physical occlusion by secondary precipitates and leached layers. A comparison in changes in surface roughness with time indicates that about a third of the decrease in reaction rate with time is attributed to increases in the intrinsic physical surface area.

Extrinsic features include processes that impact chemical weathering rate over time but are external to the silicate substrate. As such, these factors are the most difficult to re-create in laboratory experiments. The differences in reaction affinities are one important reason for lower natural weathering rates compared to experimental rates. Experimental rates are measured with high fluid/mineral ratios reacted over short times. These laboratory experiments produce solutions that are far from thermodynamic saturation with respect to the reactive phase as was shown for the Panola experiments. In contrast, natural weathering involves much lower fluid/mineral ratios reacted over much longer times. This produces pore and groundwaters closer to thermodynamic saturation as previously determined for the Panola regolith. For natural weathering, large increases in time continue to increase weathering intensities and further decrease permeabilities and reaction affinities, leading to further declines in natural weathering rates with time. For weathering under close-to-equilibrium conditions, such as occurring in many field settings, transport control will become important for weathering.

The different reaction rates observed for plagioclase in the Panola Granite illustrates that weathering is a combination of both intrinsic and extrinsic processes. The fact that naturally weathered granite reacts in the

laboratory orders of magnitude slower than in the field points to an extrinsic control, which this study has related to differences in thermodynamic saturation of column effluents relative to natural groundwater. In contrast, the reaction rate of the weathered Panola plagioclase is an order of magnitude slower than the fresh granite under essentially identical laboratory (extrinsic) conditions. This difference must be attributed to intrinsic differences in the minerals, related to differences in defect densities and the presence of surface coatings. The sum effect of these phenomena produces trends in Panola plagioclase weathering rates with time that can be described in a consistent manner by a power function. The fact that similar functions describe a group of different silicate minerals over much longer time periods suggest commonality of such processes and their usefulness in predicting the effect of time on rates of silicate weathering.

Acknowledgements

The authors would like to thank Davison Vivit of the U.S. Geological Survey for assistance in the Panola column experiments and Pete Sak of Penn State for useful discussions. The paper benefited by insightful reviews by James Drever, Harold Sverdup and Suzanne Anderson. The Water, Energy and Biogeochemical Balance Program of the U.S.G.S. funded that portion of the study. S.L.B. cites support from the Department of Energy Office of Basic Energy Sciences (DE-FG02-01ER14547). [EO]

References

- Acker, J.G., Bricker, O.P., 1992. The influence of pH on biotite dissolution and alteration kinetics at low temperature. *Geochim. Cosmochim. Acta* 56, 3073–3092.
- Anbeek, C., 1992. Surface roughness of minerals and implications for dissolution studies. *Geochim. Cosmochim. Acta* 56, 1461–1469.
- Banfield, J.F., Barker, W.W., 1994. Direct observation of reactant–product interfaces formed in natural weathering of exsolved, defective amphibole to smectite: evidence for episodic, isovolumetric reactions involving structural inheritance. *Geochim. Cosmochim. Acta* 58, 1419–1429.
- Banfield, J.F., Eggleton, R.A., 1990. Analytical transmission electron microscope studies of plagioclase, muscovite and K-feldspar weathering. *Clays Clay Miner.* 38, 77–89.

- Benedetti, M.F., Menard, O., Noack, Y., Carvalho, A., Nahon, D., 1994. Water–rock interactions in tropical catchments: field rates of weathering and biomass impact. *Chem. Geol.* 118, 203–220.
- Berner, R.A., Holdren, G.R., 1977. Mechanism of feldspar weathering: some observational evidence. *Geology* 5, 369–372.
- Bierman, P., Gillespie, A., Caffee, M., Elmore, D., 1995. Estimating erosion rates and exposure ages with ^{36}Cl produced by neutron activation. *Geochim. Cosmochim. Acta* 59, 3779–3798.
- Blum, A.E., Lasaga, A.C., 1987. Monte Carlo simulations of surface reaction rate laws. In: Stumm, W. (Ed.), *Aquatic Surface Chemistry*. Wiley, New York, pp. 255–291.
- Blum, A.E., Stillings, L.L., 1995. Feldspar dissolution kinetics. In: White, A.F., Brantley, S.L. (Eds.), *Chemical Weathering Rates of Silicate Minerals*. Mineralogical Society of America, vol. 31, pp. 291–351.
- Brantley, S.L., 1992. Kinetics of dissolution and precipitation—experimental and field results. Kharaka, Y., Maest, A. (Eds.), *Water–Rock Interaction*, vol. 7, pp. 465–469. Park City.
- Brantley, S.L., Chen, Y., 1995. Chemical weathering rates of pyroxenes and amphiboles. In: White, A.F., Brantley, S.L. (Eds.), *Chemical Weathering Rates of Silicate Minerals*. Reviews in Mineralogy, vol. 31, pp. 119–172.
- Brantley, S.L., Crane, S.R., Crear, D., Hellmann, R., Stallard, R., 1986. Dissolution at dislocation etch pits in quartz. *Geochim. Cosmochim. Acta* 50, 2349–2361.
- Brantley, S.L., Blai, A.C., Cremens, D.L., MacInnis, I., Darmody, R.G., 1993. Natural etching rates of feldspar and hornblende. *Aquat. Sci.* 55, 262–272.
- Brantley, S.L., White, A.F., Hodson, M.E., 1999. Surface areas of primary silicate minerals. In: Jamtveit, B., Meakin, P. (Eds.), *Growth, Dissolution and Pattern Formation in Geosystems*. Kluwer Academic Publishing, Amsterdam, pp. 291–326.
- Burch, T.E., Nagy, K.L., Lasaga, A.C., 1993. Free energy dependence of albite dissolution kinetics at 80 °C and pH 8.8. *Chem. Geol.* 105, 137–162.
- Busenberg, E., Clemency, C.V., 1976. The dissolution kinetics of feldspars at 25 °C and 1 atm. CO_2 partial pressure. *Geochim. Cosmochim. Acta* 40, 41–49.
- Casey, W.H., Ludwig, C., 1995. Silicate mineral dissolution as a ligand exchange reaction. In: White, A.F., Brantley, S.L. (Eds.), *Chemical Weathering Rates of Silicate Minerals*. Reviews in Mineralogy, vol. 31. Mineralogical Soc. Amer., Washington, D.C., pp. 87–117.
- Casey, W.H., Banfield, J.F., Westrich, H.R., Mclaughlin, L., 1993. What do dissolution experiments tell us about natural weathering. *Chem. Geol.* 105, 1–15.
- Chen, Y., Brantley, S.L., 1997. Temperature- and pH-dependence of albite dissolution rate at acid pH. *Chem. Geol.* 135, 275–292.
- Chou, L., Wollast, R., 1984. Study of the weathering of albite at room temperature and pressure with a fluidized bed reactor. *Geochim. Cosmochim. Acta* 48, 2205–2217.
- Clayton, J.L., 1986. An estimate of plagioclase weathering rate in the Idaho batholith based upon geochemical transport rates. In: Colman, S.M., Dethier, D.P. (Eds.), *Rates of Chemical Weathering of Rocks and Minerals*. Academic Press, Orlando, pp. 453–466.
- Cleaves, E.T., 1993. Climatic impact on isovolumetric weathering of a coarse-grained schist in the northern Piedmont Province of the central Atlantic states. *Geomorphology* 8, 191–198.
- Clow, D.W., Drever, J.I., 1996. Weathering rates as a function of flow through an alpine soil. *Chem. Geol.* 132, 131–141.
- Cygan, R.T., Casey, W.H., Boslough, M.B., Westrich, H.R., Carr, M.J., Holdren Jr., G.R., 1989. Dissolution kinetics of experimentally shocked silicate minerals. *Chem. Geol.* 78, 229–244.
- Dorn, R., 1995. Digital processing of back-scatter electron imagery: a microscopic approach to quantifying chemical weathering. *GSA Bull.* 107, 725–741.
- Drever, J.I., Clow, D.W., 1995. Weathering rates in catchments. In: White, A.F., Brantley, S.L. (Eds.), *Chemical Weathering Rates of Silicate Minerals*. Mineral. Soc. Amer., vol. 31, pp. 463–481.
- Friedman, I., Trembour, F.W., Smith, F.L., Smith, G.I., 1994. Is obsidian hydration dating affected by relative humidity? *Quat. Res.* 28, 185–190.
- Frogner, P., Schweda, P., 1998. Hornblende dissolution kinetics. *Chem. Geol.* 151, 169–179.
- Gautier, J.M., Oelkas, E.H., Schott, J., 2001. Are quartz dissolution rates proportional to B.E.T. surface areas? *Geochim. Cosmochim. Acta* 65, 1059–1070.
- Gislason, S.R., Arnorsson, S., 1990. Saturation state of natural waters in Iceland relative to primary and secondary minerals in basalt. In: Spencer, R.J., Chou, I.M. (Eds.), *Fluid–Mineral Interaction: A Tribute to H.P. Eugster*. The Geochemical Society, St. Louis, pp. 273–393.
- Goldich, S.S., 1938. A study of rock weathering. *J. Geol.* 46, 17–58.
- Hamilton, J.P., Pantano, C.G., Brantley, S.L., 2000. Dissolution of albite glass and crystal. *Geochim. Cosmochim. Acta* 64, 2603–2615.
- Helgeson, H.C., Murphy, W.M., Aagard, P., 1984. Thermodynamic and kinetic constraints on reaction rates among minerals and aqueous solutions: II. Rate constants, effective surface area, and the hydrolysis of feldspar. *Geochim. Cosmochim. Acta* 48, 2405–2432.
- Hodson, M.E., Langan, S.J., Simon, J., 1999. The influence of soil age on calculated mineral weathering rates. *Appl. Geochem.* 14, 387–394.
- Holdren Jr., G.R., Speyer, P.M., 1987. Reaction rate–surface area relationships during the early stages of weathering: II. Data on eight additional feldspars. *Geochim. Cosmochim. Acta* 51, 2311–2318.
- Hornberger, G.M., Beven, K.J., Germann, P.E., 1990. Inferences about solute transport in macroporous forest soils from time series models. *Geoderma* 46, 249–262.
- Kalinowski, B.E., Schweda, P., 1996. Kinetics of muscovite, phlogopite and biotite dissolution and alteration at pH 1–4, room temperature. *Geochim. Cosmochim. Acta* 60, 367–385.
- Kenoyer, G.J., Bowser, C.J., 1992. Groundwater chemical evolution in a sandy silicate aquifer in Northern Wisconsin: 2. Reaction modeling. *Water Resour. Res.* 28, 591–600.
- Kirkwood, S.E., Nesbitt, H.W., 1991. Formation and evolution of soils from an acidified watershed: Plastic Lake, Ontario, Canada. *Geochim. Cosmochim. Acta* 55, 1295–1308.
- Knauss, K.G., Wolery, T.J., 1986. Dependence of albite dissolution

- kinetics on pH and time at 25 °C and 70 °C. *Geochim. Cosmochim. Acta* 50, 2481–2497.
- Lasaga, A.C., 1998. *Kinetic Theory in the Earth Sciences*. Princeton Univ. Press, Princeton, NJ. 781 pp.
- Lasaga, A.C., Blum, A.E., 1986. Surface chemistry, etch pits and mineral–water reactions. *Geochim. Cosmochim. Acta* 50, 2363–2379.
- Lee, M.R., Hodson, M.E., Parsons, I., 1998. The role of intragranular microtextures and microstructures in chemical and mechanical weathering: direct comparisons of experimentally and naturally weathered alkali feldspars. *Geochim. Cosmochim. Acta* 62, 2771–2788.
- Letey, J., 1984. Adsorption and desorption of polymers on soil. *Soil Sci.* 158, 244–248.
- Luce, R.W., Bartlett, R.W., Parks, G.A., 1972. Dissolution kinetics of magnesium silicates. *Geochim. Cosmochim. Acta* 36, 35–50.
- Malmstrom, M.B., Banwart, S., 1997. Biotite dissolution at 25 °C: the pH dependence of dissolution rate and stoichiometry. *Geochim. Cosmochim. Acta* 61, 2779–2799.
- Mast, M.A., Drever, D.J., 1987. The effect of oxalate on the dissolution rates of oligoclase and tremolite. *Geochim. Cosmochim. Acta* 51, 2559–2568.
- Mellott, N.P., Brantley, S.L., Pantano, C.G., 2002. Topography of polished plates of albite crystal and glass during dissolution. In: Hellmann, R., Wood, S.A. (Eds.), *Water–Rock Interaction, Ore Deposits, and Environmental Geochemistry: A Tribute to David A. Crerar*. The Geochemical Society, Spec. Publ., vol. 7, pp. 83–95.
- Mogk, D.W., Locke, W.W.I., 1988. Application of auger electron spectroscopy (AES) to naturally weathered hornblende. *Geochim. Cosmochim. Acta* 52, 2537–2542.
- Moulton, K.L., Berner, R.A., 1998. Quantification of the effect of plants on weathering: studies in Iceland. *Geology* 26, 895–898.
- Muir, I.J., Bancroft, G.M., Nesbitt, H.W., 1989. Characteristics of altered labradorite by SIMS and XPS. *Geochim. Cosmochim. Acta* 53, 1235–1241.
- Murphy, S.F., Brantley, S.L., Blum, A.E., White, A.F., Dong, H., 1998. Chemical weathering in a tropical watershed, Luquillo Mountains, Puerto Rico: II. Rate and mechanism of biotite weathering. *Geochim. Cosmochim. Acta* 62, 227–243.
- Nesbitt, H.W., Markovics, G., 1997. Weathering of granodioritic crust, long-term storage of elements in weathering profiles, and petrogenesis of siliciclastic sediments. *Geochim. Cosmochim. Acta* 61, 1653–1670.
- Nickel, E., 1973. Experimental dissolution of light and heavy minerals in comparison with weathering and interstitial solution. *Contrib. Sedimentol.* 1, 1–68.
- Nugent, M.A., Brantley, S.L., Pantano, C.G., Maurice, P.A., 1998. The influence of natural mineral coatings on feldspar weathering. *Nature* 396, 527–622.
- Oelkers, E.H., Schott, J., Devidal, J.L., 1994. The effect of aluminum, pH, and chemical affinity on the rates of aluminosilicate dissolution reactions. *Geochim. Cosmochim. Acta* 58, 2011–2024.
- Oxburgh, R., Drever, J.I., Sun, Y.-T., 1994. Mechanism of plagioclase dissolution in acid solutions at 25 °C. *Geochim. Cosmochim. Acta* 58, 661–669.
- Paces, T., 1973. Steady-state kinetics and equilibrium between ground water and granitic rock. *Geochim. Cosmochim. Acta* 37, 2641–2663.
- Paces, T., 1986. Rates of weathering and erosion derived from mass balance in small drainage basins. In: Colman, S.L., Dethier, D.P. (Eds.), *Rates of Chemical Weathering of Rocks and Minerals*. Academic Press, Orlando, pp. 531–550.
- Parkhurst, D.L., 1997. Geochemical mole-balance modeling with uncertain data. *Water Resources Research* 33 (1957), 1970.
- Schnoor, J.L., 1990. Kinetics of chemical weathering: a comparison of laboratory and field rates. In: Stumm, W. (Ed.), *Aquatic Chemical Kinetics*. Wiley, New York, pp. 475–504.
- Schweda, P., 1989. Kinetics of alkali feldspar dissolution at low temperature. In: Miles, D.L. (Ed.), *Proc. 6th Intern. Symp. Water/Rock Interaction*, Malver. A.A. Balkema, Rotterdam, pp. 609–612.
- Siegal, D., Pfannkuch, H.O., 1984. Silicate mineral dissolution at pH 4 and near standard temperature and pressure. *Geochim. Cosmochim. Acta* 48, 197–201.
- Smeck, N.E., Ciolkosz, E.J., 1989. Fragipans: their occurrence, classification and genesis. *SSSA Spec. Publ.*, vol. 24. Soil Sci. Soc. Amer., Madison. 153 pp.
- Stefansson, A., 2001. Dissolution of primary minerals of basalt in natural waters I. Calculation of mineral solubilities from 0 °C to 350 °C. *Chem. Geol.* 172, 225–250.
- Stewart, B.W., Capo, R.C., Chadwick, O.A., 2001. Effects of rainfall on weathering rate, base cation provenance, and Sr isotope composition of Hawaiian soils. *Geochim. Cosmochim. Acta* 65, 1087–1099.
- Stillings, L.L., Brantley, S.L., 1995. Feldspar dissolution at 25 °C and pH 3: reaction stoichiometry and the effect of cations. *Geochim. Cosmochim. Acta* 59, 1483–1496.
- Stillings, L.L., Drever, J.I., Brantley, S., Sun, Y., Oxburgh, R., 1996. Rates of feldspar dissolution at pH 3–7 with 0–8 M oxalic acid. *Chem. Geol.* 13, 79–89.
- Stonestrom, D.A., White, A.F., Akstin, K.C., 1998. Determining rates of chemical weathering in soils–solute transport versus profile evolution. *J. Hydrol.* 209, 331–345.
- Suarez, D.L., Wood, J.D., 1995. Short-term and long term weathering rates of a feldspar fraction isolated from an arid zone soil. *Chem. Geol.* 132, 143–150.
- Sverdrup, K., Warfvinge, P., 1995. Estimating field weathering rates using laboratory kinetics. In: White, A.F., Brantley, S.L. (Eds.), *Chemical Weathering Rates of Silicate Minerals*. Reviews in Mineralogy, vol. 31. Mineral. Soc. Amer., Washington, D.C., pp. 485–541.
- Swoboda-Colberg, N.G., Drever, J.I., 1992. Mineral dissolution rates: a comparison of laboratory and field studies. In: Kharaka, Y.K., Maest, A.S. (Eds.), *Proc. 7th Intern. Symp. Water–Rock Interaction*. Balkema, Park City, UT, pp. 115–117.
- Swoboda-Colberg, N.G., Drever, J.D., 1993. Mineral dissolution rates in plot-scale field and laboratory experiments. *Chem. Geol.* 105, 51–69.
- Taylor, A., Blum, J.D., 1995. Relation between soil age and silicate weathering rates determined from the chemical evolution of a glacial chronosequence. *Geology* 23, 979–982.
- Taylor, A.S., Blum, J.D., Lasaga, A.C., 2000a. The dependence of

- labradorite dissolution and Sr isotope release rates on solution saturation state. *Geochim. Cosmochim. Acta* 64, 2389–2400.
- Taylor, A.S., Blum, J.D., Lasaga, A.C., MacInnis, I.N., 2000b. Kinetics of dissolution and Sr release during biotite and phlogopite weathering. *Geochim. Cosmochim. Acta* 64, 1191–1208.
- Tisdall, J.M., Oades, H., 1982. Organic matter and water-stable aggregates in soils. *J. Soil Sci.* 3, 141–163.
- van Grinsven, J.J.M., van Riemsdijk, W.H., 1992. Evaluation of batch and column techniques to measure weathering rates in soils. *Geoderma* 52, 41–57.
- van Hees, P.A.W., Lundstrom, U.S., Morth, C.M., 2002. Dissolution of microcline and labradorite in a forest O horizon extract: the effects of naturally occurring organic acids. *Chem. Geol.* 189, 199–211.
- Velbel, M.A., 1985. Geochemical mass balances and weathering rates in forested watersheds of the southern Blue Ridge. *Am. J. Sci.* 2, 904–930.
- Velbel, M.A., 1993. Constancy of silicate mineral weathering ratios between natural and experimental weathering: implications for hydrologic control of differences in absolute rate. *Chem. Geol.* 105, 89–99.
- Welch, S.A., Ullman, W.J., 1993. The effect of organic acids on plagioclase dissolution rates and stoichiometry. *Geochim. Cosmochim. Acta* 57, 225–2736.
- Welch, S.A., Ullman, W.J., 1996. Feldspar dissolution in acidic and organic solutions: compositional and pH dependence of dissolution rate. *Geochim. Cosmochim. Acta* 60, 2939–2948.
- White, A.F., 1995. Chemical weathering rates in soils. In: White, A.F., Brantley, S.L. (Eds.), *Chemical Weathering Rates of Silicate Minerals*. Mineralogical Soc. Amer., vol. 31, pp. 407–458.
- White, A.F., 2002. An integrated approach for determining mineral weathering rates based on regolith solute and solute elemental gradients: application to biotite weathering in Saprolites. *Chem. Geol.* 190, 69–89.
- White, A.F., Blum, A.E., 1995. Effects of climate on chemical weathering rates in watersheds. *Geochim. Cosmochim. Acta* 59, 1729–1747.
- White, A.F., Brantley, S.L. (Eds.), 1995. *Chemical Weathering Rates of Silicate Minerals*. Reviews in Mineralogy, vol. 31. Mineralogical Society of America, Washington, D.C. 584 pp.
- White, A.F., Hochella Jr., M.F., 1992. Surface chemistry associated with the cooling and subaerial weathering of resented basalt flows. *Geochim. Cosmochim. Acta* 56, 3711–3721.
- White, A.F., Peterson, M.L., 1990. Role of surface area characterization in geochemical models. In: Melchior, R.L., Bassett, R. (Eds.), *Chemical Modeling of Aqueous Systems II*. Amer. Chem. Soc. Symp. Ser., vol. 416, pp. 461–475.
- White, A.F., Blum, A.E., Schulz, M.S., Bullen, T.D., Harden, J.W., Peterson, M.L., 1996. Chemical weathering of a soil chronosequence on granitic alluvium: 1. Reaction rates based on changes in soil mineralogy. *Geochim. Cosmochim. Acta* 60, 2533–2550.
- White, A.F., Bullen, T.D., Vivit, D.V., Schulz, M.S., 1999a. The role of disseminated calcite in the chemical weathering of granitoid rocks. *Geochim. Cosmochim. Acta* 63, 1939–1999.
- White, A.F., Blum, A.E., Bullen, T.D., Vivit, D.V., Schulz, M., Fitzpatrick, J., 1999b. The effect of temperature on experimental and natural weathering rates of granitoid rocks. *Geochim. Cosmochim. Acta* 63, 3277–3291.
- White, A.F., Bullen, T.D., Schulz, M.S., Blum, A.E., Huntington, T.G., Peters, N.E., 2001. Differential rates of feldspar weathering in granitic regoliths. *Geochim. Cosmochim. Acta* 65, 847–869.
- White, A.F., Blum, A.E., Schulz, M.S., Huntington, T.G., Peters, N.E., 2002. Chemical weathering of the Panola Granite: Solute and regolith elemental fluxes and the dissolution rate of biotite. In: Hellmann, R., Wood, S.A. (Eds.), *Water–Rock Interaction, Ore Deposits, and Environmental Geochemistry: A Tribute to David A. Crerar*. The Geochemical Society, Spec. Publ., vol. 7, pp. 37–59.
- Yau, S., 1999. Dissolution kinetics of feldspar in the Cape Cod aquifer, Massachusetts: calculation of groundwater residence times. Master's thesis, Pennsylvania State University. 95 pp.
- Zhang, H., Bloom, P.R., 1999. The pH dependence of hornblende dissolution. *Soil Sci.* 164, 624–632.
- Zhang, H., Bloom, P.R., Nater, E.A., Erich, M.S., 1996. Rates and stoichiometry of hornblende dissolution over 115 days of laboratory weathering at pH 3.6–4.0 and 25 °C in M lithium acetate. *Geochim. Cosmochim. Acta* 60, 941–950.